Available online at www.sciencedirect.com

ScienceDirect

Biochimica et Biophysica Acta 1767 (2007) 1073–1101

Biochimica et Biophysica Acta BBA

www.elsevier.com/locate/bbabio

Review

Infrared spectroscopy of proteins

Andreas Barth *

Department of Biochemistry and Biophysics, The Arrhenius Laboratories for Natural Sciences, Stockholm University, S-106 91 Stockholm, Sweden

Received 5 January 2007; received in revised form 18 June 2007; accepted 19 June 2007
Available online 28 June 2007

Abstract

This review discusses the application of infrared spectroscopy to the study of proteins. The focus is on the mid-infrared spectral region and the study of protein reactions by reaction-induced infrared difference spectroscopy.

Keywords: Infrared spectroscopy; FTIR; Protein; Protein structure; Protein function; Secondary structure; Water; Amide I; Amino acid side chain; Enzyme activity; Difference spectroscopy

1. Introduction

Infrared spectroscopy is one of the classical methods for structure determination of small molecules. This standing is due to its sensitivity to the chemical composition and architecture of molecules. The *high information content* in an infrared spectrum carries over also to biological systems. This makes infrared spectroscopy a valuable tool for the investigation of protein structure [1–11] of the molecular mechanism of protein reactions [2,10–35] and of protein folding, unfolding and misfolding [7,10,36–44]. The wealth of information in the infrared spectrum can be exploited even for biological systems that are larger than proteins [45–49]. A striking example is the possibility to identify bacterial strains from the infrared spectrum and to differentiate and classify microorganisms [45].

Further advantages of infrared spectroscopy are a *large application range* from small soluble proteins to large membrane proteins, a *high time resolution* down to 1 μs with moderate effort, often a *short measuring time*, the *low amount of sample* required (typically 10–100 μg) and the relatively *low costs* (top class spectrometers for 40 000 € or $). These advantages for protein research are widely recognised in the academic world, but, surprisingly, the breakthrough of infrared spectroscopy in commercial protein analysis has still to come.

This review discusses the application of infrared spectroscopy to the study of proteins. The focus is on the mid-infrared spectral region and the study of protein reactions by reaction-induced infrared difference spectroscopy.

2. Absorption of infrared light

The absorption of infrared radiation excites vibrational transitions of molecules. In the mid- and far-infrared spectral regions this is generally the case when the frequencies of light and vibration are equal and when the molecular dipole moment changes during the vibration. Since vibrational frequency and probability of absorption depend on the strength and polarity of the vibrating bonds, they are influenced by intra- and intermolecular effects. The approximate position of an infrared absorption band is determined by the vibrating masses and the type of bond (single, double, triple), the exact position by electron withdrawing or donating effects of the intra- and intermolecular environment and by coupling with other vibrations. The strength of absorption increases with increasing polarity of the vibrating bonds. In protein science, the effect of the environment on vibrational frequencies is often a telltale of how proteins work.

Basically all polar bonds contribute to the infrared absorption. This is at the same time the crux and the strength of infrared

Abbreviations: ATR, attenuated total reflection; δ, in plane bending vibration; FTIR, Fourier transform infrared; IR, infrared; γ_w, wagging vibration; γ_t, twisting vibration; γ_r, rocking vibration; ε, extinction coefficient; NMA, *N*-methylacetamide; ν, stretching vibration; ν_s, symmetric stretching vibration; ν_{as}, antisymmetric stretching vibration; TDC, transition dipole coupling; TDM, transition dipole moment

* Tel.: +46 8 162452; fax: +46 8 155597.
E-mail address: Andreas.Barth@dbb.su.se.

0005-2728/$ - see front matter © 2007 Elsevier B.V. All rights reserved.
doi:10.1016/j.bbabio.2007.06.004

spectroscopy—a crux, because the spectrum of larger molecules is composed of many overlapping bands with the consequence that much information can be hidden under broad, featureless absorption bands; a strength, because nearly all biomolecules absorb infrared radiation. The latter brings with it that there is no need to label biomolecules to make them detectable. This notion of infrared spectroscopy being a marker-free technique has recently received an interesting twist in a study that reported a genetically encoded CN infrared label which was used to probe ligand binding to myoglobin [50].

The infrared spectrum is plotted against the inverse of the wavelength, the *wavenumber* $\tilde{\nu}$, which is proportional to the transition energy and has the unit cm^{-1}. The horizontal coordinate of the spectrum runs from high wavenumbers to low wavenumbers according to a recommendation of the International Union of Pure and Applied Chemistry (IUPAC) [51,52]. This is equivalent to running from small wavelength to large wavelength as usual in ultraviolet-visible spectroscopy. The convention is particularly important for the near-infrared spectral range where some spectra are plotted against wavelength and others against wavenumber.

The infrared spectral region is adjacent to the visible spectral region and extends from 0.78 μm to about 1000 μm. It can be further subdivided into the *near-infrared* region from 780 nm to 2.5 μm, the *mid-infrared* region from 2.5 μm to 50 μm and the *far-infrared* region from 50 μm to 1000 μm. The latter region is also called *terahertz* frequency regime. The mid-infrared spectral range extending from 2.5 to 50 μm corresponds to 4000 to 200 cm^{-1}, which corresponds to frequencies of 10^{13} to 10^{14} Hz. Thermal energy kT at room temperature corresponds to $\sim 200\ cm^{-1}$ implying that absorption in the mid-infrared spectral range is generally from the vibrational ground state the first excited vibrational state.

Infrared spectroscopy is one variant of vibrational spectroscopy. Other variants are Raman spectroscopy, reviewed in refs. [53–61], and photoacoustic spectroscopy which provide essentially the same information. Thus, some of the examples in the next section are from Raman studies.

3. Information that can be derived from the infrared spectrum

3.1. Chemical structure of the vibrating group

The chemical structure of a molecule is the dominating effect that determines vibrational frequencies via the strengths of the vibrating bonds and the masses of the vibrating atoms. In spite of that, the chemical structure of a protein cannot be deduced from the infrared spectrum because of many overlapping bands. Changes in chemical structure however can be detected and an important example is a change of protonation state of side chains which is often essential for protein function. Here, infrared spectroscopy seems to be the method of choice since the protonation state of most side chains is reflected in the spectrum. Some examples are: protonation of Asp and Glu residues accompanies proton pumping by bacteriorhodopsin [14–17,23], electron transfer reactions [12,13], Ca^{2+} release from the Ca^{2+} ATPase [62] and seems to provide a mechanism of charge compensation when the negatively charged ATP binds to the Ca^{2+}-ATPase [63]. As for Asp and Glu residues, the protonation state of other catalytically active side chains can be characterised by infrared spectroscopy, as done for example for His and Tyr residues of photosystem II [64,65] and bacteriorhodopsin [66–68].

Other examples for an alteration of chemical structure that can be monitored by infrared spectroscopy are protein modifications like phosphorylation [69,70] and chemical reactions catalysed by enzymes [71–78], reviewed in Ref. [27].

3.2. Chemical properties of neighbouring groups in a molecule

The electron density of a given bond in a molecule is influenced by neighbouring groups within the molecule via inductive and mesomeric effects. The latter is the reason for amide groups absorbing at lower wavenumbers than carbonyl groups of carboxylic acids [79].

3.3. Redox state

Redox reactions are the basis of the energy delivering processes in living organisms. They affect the electron density distribution of a given molecule and thus will alter its vibrational spectrum. This is illustrated well by model studies on isolated biological cofactors involved in photosynthesis [80–83] that allowed the assignment of signals in the protein spectra to specific molecular groups of the cofactors and in consequence statements about their protein environment [12,13, 21,22].

3.4. Bond parameters

As pointed out by Deng and Callender [53], vibrational spectroscopy is exceptionally sensitive to changes in bond strength since a change of 0.02% can be easily detected. As bond strength and bond length are directly related [59,84–86], bond distortions smaller than 1 pm in the course of a catalytic reaction can be monitored with astonishing accuracy. Deng and Callender concluded: “although an oversimplification, it can be said that the resolution of vibrational spectroscopy picks up where diffraction and multidimensional nuclear magnetic resonance (NMR) techniques leave off, at ca. 0.2 Å, and extends down to much lower lengths”. The sensitivity to bond parameters has been exploited in quantitative studies of, for example, chymotrypsins [87,88], subtilisins [87], myosin [89], Ras [90–92], and Ca^{2+}-ATPase [93,94].

3.5. Bond angles and conformation

Vibrations in adjacent parts of a molecule are often coupled and this coupling depends on details of the molecular geometry. Therefore, coupling can provide insight into the three-dimensional structure of molecules. Examples are (i) the two coupled CO vibrations in the COO^- group which make the carboxylate absorption sensitive to the mode of cation chelation [95–97] and has been used in studies of several Ca^{2+} binding proteins [98,99]; (ii) the sensitivity of P−O or V−O stretching vibrations of phosphates or vanadates on the bond angle [100], applied to

myosin [89] and Ras [90,91] studies; and (iii) transition dipole coupling of the amide groups of the protein backbone which makes this mode sensitive to the 3D structure of the backbone.

3.6. Hydrogen bonding

Hydrogen bonds stabilize the structure of proteins and are essential for catalysis. Vibrational spectroscopy is one of the few methods that directly report on the strength of hydrogen bonds. As a general rule, hydrogen bonding lowers the frequency of stretching vibrations, since it lowers the restoring force, but increases the frequency of bending vibrations since it produces an additional restoring force [79]. Formation of a single hydrogen bond to a C═O group leads to a 20 cm^{-1} down shift for the methylacetate–water complex in an argon matrix [101,102] and of 25 cm^{-1} for propionic acid in an ethanol/hexane (1:200) mixture [103].

Hydrogen bonding to PO_2^- groups lowers the observed band position of the symmetric stretching vibration by 3 to 20 cm^{-1} and of the antisymmetric stretching vibration by 20–34 cm^{-1} [104–107] with a single hydrogen bond contributing 16 cm^{-1} in a nitrogen matrix [107]. This is due to two effects [106]: (i) less electron density in the P − O bonds and (ii) a relaxation of phosphate geometry towards the ideal tetrahedron form due to the reduced Coulomb repulsion.

For the quantitative evaluation of band shifts induced by hydrogen bonding Badger and Bauer relationships [108] are often used. These are linear dependencies between the enthalpy of hydrogen bond formation ΔH and the frequency of stretching vibrations [53,59,109,110]. For the carbonyl group of methyl acetate, a model for Asp and Glu, a downshift of 1 cm^{-1} corresponds to a favourable binding enthalpy of approximately 1.7 kJ/mol [53,59,110]. In Raman studies [54], favourable binding enthalpies with respect to water as large as −60 kJ/mol have been detected for C═O groups of substrates bound to enzymes.

3.7. Electric fields

Similar to hydrogen bonding, the electric field produced by the environment modifies the electron density distribution of a vibrating group. A strong electric field has been detected for example in the active site of dehalogenase where it polarises the product of the catalytic reaction [55]. For carboxyl groups in the absence of hydrogen bonding (bands above 1740 cm^{-1}), there is an inverse correlation of the C═O stretching frequency with the dielectric constant ε [103].

3.8. Conformational freedom

Besides band position and band intensity, the third spectral parameter, the band width, is also informative. Due to its short characteristic time scale on the order of 10^{-13} s, vibrational spectroscopy provides a snapshot of the sample conformer population. As the band position for a given vibration usually is slightly different for every conformer, heterogeneous band broadening is the consequence. Flexible structures will thus give broader bands than rigid structures and the band width is a measure of conformational freedom. It is possible to relate band width with entropy and thus to quantify entropic effects in catalysis [53]. Motional narrowing can counteract the effects of a heterogeneous environment for amide groups that are hydrogen bonded to bulk water [111–113].

For molecules that bind to proteins, the restriction of conformational freedom is a natural consequence of binding. This often reduces the band width by a factor of two [27]. The band width has been interpreted in studies of nucleotide binding to Ras [90,114], ubiquinone binding to cytochrome bo_3 [115], substrate analogue binding to lactate dehydrogenase [53], nicotinamide dinucleotide binding to transhydrogenase [116], and of the phosphorylated Asp residue of the sarcoplasmic reticulum Ca^{2+}-ATPase [69].

4. Infrared spectrometers

4.1. Fourier transform infrared spectrometers

Modern infrared spectrometers are usually *Fourier transform infrared (FTIR) spectrometers*. Their name originates from the fact that the detector signal of these spectrometers is related by a Fourier transformation to the measured spectrum. The heart of an FTIR spectrometer is an interferometer, like the Michelson interferometer shown in Fig. 1. It has a fixed and a movable mirror. The latter generates a variable optical path difference between two beams which gives a detector signal that contains the spectral information. Light emitted from the light source is split by a beam splitter: about half of it is reflected towards the fixed mirror and from there reflected back towards the beamsplitter where about 50% passes to reach the detector (black arrows in Fig. 1). The other half of the initial light intensity passes the beam splitter on its first encounter, is reflected by the movable mirror back to the beamsplitter where 50% of it is reflected towards the detector (grey arrows in Fig. 1). When the two beams recombine they interfere and there will be constructive or destructive interference depending on the optical path difference d. The instrument measures the light intensity relative to the position of the movable mirror and this is called an *interferogram*. It turns out that the interferogram is the Fourier transform of the spectrum. A second Fourier transform performed by a computer converts the measured data back into a spectrum. In total, a Fourier transform spectrometer performs two Fourier transformations: one by the interferometer, one by the computer.

That the interferometer produces the Fourier transform of the spectrum is best seen when a monochromatic source is considered. Its spectrum $S(\lambda)$ is described by a delta function located at λ_0. Depending on the position of the movable mirror one obtains constructive or destructive interference at the detector and the detector signal $I(d)$ varies as a cosine function with the mirror position which determines the optical path difference d. This cosine function and the delta function describing the monochromatic spectrum are related by a Fourier transformation. Thus, a second Fourier transformation performed by the computer generates the spectrum $S(\lambda)$.

The main advantage of Fourier transform spectrometers is the rapid data collection and high light intensity at the detector

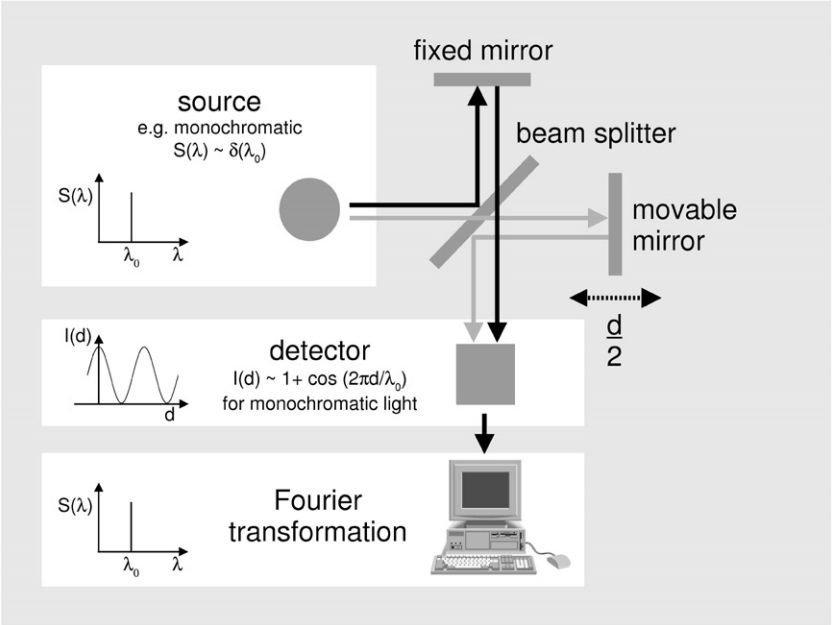

Fig. 1. Scheme of a Fourier transform infrared spectrometer. See text for further explanation. Republished from [11]. © 2006 Nova Science Publishers.

and in consequence the high signal to noise ratio. Therefore a spectrum can be recorded in as few as 10 ms. Different types of detectors, light sources and other optical components are used in different regions of the infrared spectral range.

4.2. Dispersive infrared spectrometers

Dispersive infrared spectrometers are no longer used for routine measurements but are still valuable for special applications like time-resolved measurements. Briefly, a dispersive infrared spectrometer consists of a light source, optics (often mirrors) that focus the light on the sample and then on the entrance slit of a monochromator, a monochromator, another mirror to focus the light on a detector and a detector. The positioning of the monochromator behind the sample avoids the detection of heat radiation from the sample. The disadvantage of these instruments is that the incident light is split into its spectral components. Therefore the light intensity reaching the detector is low, which results in a signal to noise ratio that is much worse than that of Fourier transform infrared spectrometers.

5. Sampling techniques

5.1. Transmission measurements

In transmission measurements, the infrared light passes a cuvette containing the sample before it reaches the detector. If the sample is homogeneous, it absorbs light according to the Beer–Lambert law

$$A(\tilde{\nu}) = \log(I_0/I) = c\varepsilon(\tilde{\nu})d$$

where A is the absorbance, I_0 the light intensity before the sample, I the light intensity after the sample, c the concentration of the absorbing substance, ε the molar absorption index or extinction coefficient and d the pathlength. ZnSe, BaF_2 and CaF_2 cuvettes are often used, the latter two have the advantage that excitation with UV light is possible. A simple demountable infrared cuvette consists either of two plane windows separated by a spacer that defines the pathlength or of one plane window and a window with a trough. Recently, a number of flow cells have been developed that enable mixing experiments [36,117–119].

One drawback of infrared spectroscopy of aqueous solutions is the strong absorbance of water in the mid-infrared spectral region (near 1645 cm^{-1}) [120] which overlaps the important amide I band of proteins and some side chain bands (see below). When these protein bands are of interest, the strong water absorption demands a short path length for aqueous samples, which is typically around 5 μm, and in turn relatively high concentrations. Using ^2H_2O, the pathlength can be increased to 50 μm and the concentration lowered because the water band is downshifted to ~1210 cm^{-1}. Typical concentrations in infrared spectroscopy are 0.1 to 1 mM for proteins and 1 to 100 mM for small molecules. However, concentrations as low as 0.3 mg/ml have been reported [121] and the amount of protein required is low because of the small sample volume, typically in the 10–100 μg range, and can be as low as 50 ng [122]. A promising technique to further reduce the amount of material is surface-enhanced infrared spectroscopy [123]—the infrared analog of surface enhanced Raman spectroscopy. It enables studies of protein monolayers because protein absorption is enhanced by typically a factor of 100 when the protein is absorbed on a film or suspension of metal particles. Possible disadvantages are the sensitivity of band intensities on the structure of the metal surface and structural modifications due to protein interaction with the metal surface.

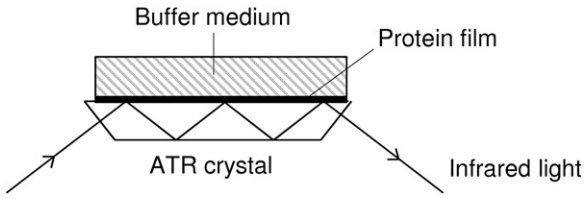

Fig. 2. A typical ATR setup. Republished from [11]. © 2006 Nova Science Publishers.

5.2. Attenuated total reflectance

The attenuated total reflectance (ATR) technique [26,124–126] is illustrated in Fig. 2. Compared to transmission experiments, it avoids the handling problems which are caused by the required short pathlength. In an ATR experiment a sample is placed on a crystal with an index of refraction that is larger than that of the sample and typically larger than 2. Infrared light is coupled into the crystal and directed towards the sample interface at such an angle of incidence that it is totally reflected at the interface between sample and crystal. After one or several reflections the measuring light leaves the crystal and is focused on the detector. Upon reflection at the interface between sample and crystal, light penetrates into the sample. This so-called evanescent wave has the same frequency as the incoming light but the amplitude of the electric field decays exponentially with the distance from the interface. The evanescent wave may be absorbed by the sample and thus the light reaching the detector carries the information about the infrared spectrum of the sample. The penetration depth is on the order of the wavelength, which means that the optical thickness of the sample is small enough for measurements of aqueous solutions. The penetration depth depends also on the angle of incidence and the ratio of the indices of refraction of crystal and sample.

For protein samples, usually a protein film is prepared on the crystal surface [121,125,127,128], often simply by drying, and a buffer is placed on top of the film. The thickness of the buffer layer does not influence the measured spectrum. The advantage of the method is that often the buffer can be exchanged without disturbing the film. This makes sample manipulations relatively simple and makes the method very flexible. The disadvantage is that the preparation of a stable film can be difficult and sometimes impossible. The film might also detach when the buffer is exchanged.

For these difficult cases and for soluble proteins it is advantageous to separate a sample compartment close to the ATR crystal from a reservoir by a dialysis membrane. In this way the medium in the reservoir can be altered without disturbing the protein sample in the sample compartment [129–132].

6. Time-resolved infrared spectroscopy

6.1. Overview

Three of the most common time-resolved infrared techniques that have been applied to study proteins will be briefly discussed here: the rapid scan technique, the step scan technique and single wavelength measurements. The former two are performed on FTIR spectrometers, while the latter is done on a dispersive instrument. Not discussed here will be the pump-probe technique and stroboscopic Fourier transform infrared spectroscopy. All techniques mentioned and biological or photochemical applications thereof have been reviewed before [20,23,133–143].

6.2. The rapid scan technique

In the rapid scan technique the movable interferometer mirror is moved at a maximum speed of 10 cm/s. From one complete forward and backward movement of the mirror, up to 4 spectra can be obtained which results in a maximum time resolution of about 10 ms at 12 cm^{-1} optical resolution. A single experiment can yield a full series of time-resolved spectra.

6.3. The step scan technique

Data recording in an FTIR spectrometer is not continuous but done at discrete positions of the movable mirror. In the step scan technique the movement of the movable mirror is stopped at these positions, a time-resolved experiment performed and the time course of intensity at the detector recorded. Then the mirror is moved to the next position and the experiment is repeated. One obtains a series of time-resolved intensity measurements at the different mirror positions. When intensity data of all mirror positions at a given time are combined, one obtains the interferogram at that time which can be transformed into a spectrum. Accordingly all data are reshuffled to obtain a time-resolved series of interferograms which is then transformed into a series of time-resolved spectra. The time resolution of this technique can be of the order of nanoseconds and is limited by the response times of detector and electronics. A requirement for the step scan technique is that the experiment can be accurately reproduced at least several hundred times, since kinetic traces at typically about 600 mirror positions have to be sampled at 4 cm^{-1} optical resolution [144]. This requirement is either met by cyclic or reversible systems where the reaction of interest can be repeated many times with the same sample, by repeating the experiment at different small sample spots for each interferometer position [145], or by using a flow cell to conveniently refill the infrared cuvette with fresh material [146].

6.4. Single wavelength measurements

Single wavelength measurements are done on a dispersive instrument. The monochromator is set to a wavenumber of interest and the intensity change at the detector during the time-resolved experiment is recorded. The advantage of this method is that a kinetic trace can be obtained from a single experiment. However, the relatively low signal to noise ratio of dispersive instruments has the consequence that only relatively large absorbance changes ($\Delta A > 0.002–0.01$) can be resolved in a single experiment. The lower limit of sensitivity applies when the infrared band of interest is broad which allows one to increase the spectral width that is detected. The signal to noise

Table 1
Overview of amino acid side chain infrared bands

Assignments	Band position/cm^{-1}, (ε/M^{-1} cm^{-1}) in ^1H_2O	Band position/cm^{-1}, (ε/M^{-1} cm^{-1}) in ^2H_2O	Remarks
Cys, ν(SH)	2551	1849	
Asp, ν(C═O)	1716 (280)	1713 (290)	Without H-bond up to 1762 cm^{-1} observed in proteins [422]. Single H-bond shifts 25 cm^{-1} down. Above ~1740 cm^{-1} inverse correlation of ν(C═O) with ε (dielectric constant) [103]. Small down or up shifts in ^2H_2O indicate H-bonding to the hydroxyl group [386].
Glu, ν(C═O)	1712 (220)	1706 (280)	Expected to be up to 50 cm^{-1} higher without H-bond. See also Asp ν(C═O)
Asn, ν(C═O)	1677–1678 (310–330)	1648 (570)	Up to 1704 cm^{-1} in proteins [423]
Arg, $\nu_{as}(CN_3H_5^+)$	1652–1695 (420–490)	1605–1608 (460)	Position depends on the salt bridge between Arg and other residues only for ^1H_2O not for ^2H_2O. In ^1H_2O near 1672 cm^{-1} without salt bridge. In proteins up to 1695 cm^{-1} (^1H_2O) and down to 1595 cm^{-1} (^2H_2O) [155,424,425]
Gln, ν(C═O)	1668–1687 (360–380)	1635–1654 (550)	
Arg, $\nu_s(CN_3H_5^+)$	1614–1663 (300–340)	1581–1586 (500)	Position depends on the salt bridge between Arg and other residues only for ^1H_2O not for ^2H_2O. In ^1H_2O near 1635 cm^{-1} without salt bridge. In deuterated proteins up to 10 cm^{-1} lower [155,424]
$HisH_2^+$, ν(C═C)	1631 (250)	1600 (35), 1623 (16)	Only one strong band observed for 4-methylimidazole at 1633 (H_2O) and 1605 cm^{-1} (^2H_2O) [426]
Lys, $\delta_{as}(NH_3^+)$	1626–1629 (60–130)	1201	^2H_2O band position based on shift observed for CH_3NH_3Cl and $CH_3N^2H_3Cl$
Tyr-OH, ν(CC) δ(CH)	1614–1621 (85–150)	1612–1618 (160)	ε estimated relative to 1517 cm^{-1} band, Tyr or *p*-cresol
Asn, $\delta(NH_2)$	1612–1622 (140–160)		
Trp, ν(CC), ν(C═C)	1622	1618	
Tyr–O^-, ν(CC)	1599–1602 (160)	1603 (350)	Tyr or *p*-cresol
Tyr–OH, ν(CC)	1594–1602 (70–100)	1590–1591 (<50)	ε estimated relative to 1517 cm^{-1} band, Tyr or *p*-cresol
Gln, $\delta(NH_2)$	1586–1610 (220–240)	1163	
HisH, ν(C═C)	1575,1594 (70)	1569, 1575	Doublet due to the two protonated tautomers of His
Asp, $\nu_{as}(COO^-)$	1574–1579 (290–380)	1584 (820)	May shift +60/−40 cm^{-1} [96,99] upon cation chelation, in extreme cases band position as for ν(C═O) [95]
Glu, $\nu_{as}(COO^-)$	1556–1560 (450–470)	1567 (830)	See Asp $\nu_{as}(COO^-)$
Lys, $\delta_s(NH_3^+)$	1526–1527 (70–100)	1170	^2H_2O band position based on shift observed for CH_3NH_3Cl and $CH_3N^2H_3Cl$ [427]
Tyr–OH, ν(CC), δ(CH)	1516–1518 (340–430)	1513–1517 (500)	Tyr or *p*-cresol
Trp, ν(CN), δ(CH), δ(NH)	1509		Indole infrared spectrum
Tyr–O^-, ν(CC), δ(CH)	1498–1500 (700)	1498–1500 (650)	Tyr or *p*-cresol
Trp, ν(CC), δ(CH)	1496		Trp Raman spectrum, observed in the indole infrared spectrum at 1487 cm^{-1}
Phe, ν(CCring)	1494 (80)		
$\delta_{as}(CH_3)$	1445–1480		
$\delta(CH_2)$	1425–1475		Good group frequency, normally at 1463, near 1425 cm^{-1} and more intense when next to a C═O group [79]
Pro, ν(CN)	1400–1465		Sensitive to backbone conformation [428,429]
Trp, δ(CH), ν(CC), ν(CN)	1462	1455 (200)	ε estimated from comparison with he 1517 cm^{-1} Tyr band [430]
His^-, $\delta(CH_3)$, ν(CN)	1439	1439	Observed for 4-methylimidazole with a strong contribution of $\delta(CH_3)$. Thus, position for His may differ.
Trp, δ(NH), ν(CC), δ(CH)	1412–1435	1382	^1H_2O: higher number for Raman spectrum of Trp, lower number for infrared imidazole spectrum. ^2H_2O: Raman spectrum of Trp
Gln, ν(CN)	1410	1409	
Glu, $\nu_s(COO^-)$	1404 (316)	1407	See Asp $\nu_s(COO^-)$
Asp, $\nu_s(COO^-)$	1402 (256)	1404	May shift +60/−90 cm^{-1} upon cation chelation [96], in extreme cases band position as for ν(C−O) of COOH group [95]. Band position of Asp in ^2H_2O estimated from shift observed for CH_3COO^-
$\delta_s(CH_3)$	1375 or (1368, 1385)		One band for one CH_3 group, two bands for two adjacent groups (Val, Leu), narrower than $\delta_{as}(CH_3)$ but same intensity [79]. Insensitive to hydrocarbon chain conformation [431]

Table 1 (*continued*)

Assignments	Band position/cm^{-1}, (ε/M^{-1} cm^{-1}) in ^1H_2O	Band position/cm^{-1}, (ε/M^{-1} cm^{-1}) in ^2H_2O	Remarks
Trp	1352–1361		Higher number for Raman spectrum of Trp, lower number for infrared imidazole spectrum.
Trp	1334–1342	1334 (100)	^1H_2O: higher number for Raman spectrum of Trp, lower number for infrared imidazole spectrum. ^2H_2O: IR spectrum of Trp in protein
δ(CH)	1315–1350		
Trp, δ(NH), ν(CN), δ(CH)	1276		Indole infrared spectrum
Tyr–O$^-$, ν(C–O), ν(CC)	1269–1273 (580)		Tyr or *p*-cresol
Asp, Glu, δ(COH)	1264–1450	955–1058	Hydrogen bonded (1058 and 1450 cm^{-1}) and free (955 and 1264 cm^{-1}) CH_3COOH
Trp, δ(CH), ν(CC)	1245		Indole IR spectrum
Tyr–OH ν(C–O), ν(CC)	1235–1270 (200)	1248–1265 (150)	Tyr or *p*-cresol, band sensitive to H-bonding, 3 to 11 cm^{-1} lower in ^2H_2O, ε in ^2H_2O estimated from comparison with 1517 cm^{-1} band
His, δ(CH), ν(CN), δ(NH)	1217, 1229, 1199	1217, 1223, 1239	Values are for His^-, HisH and $HisH_2^+$, respectively
Trp, ν(CC)	1203		Indole infrared spectrum
Ser, δ(COH) or δ(CO^{2}H), ν(CO)	1181–1420	875–985	Band position sensitive to hydrogen bonding
γ_w(CH_2)	1170–1382		Couples with adjacent CH_2 groups [79]. Sensitive to hydrocarbon chain conformation [431]
Tyr–OH, δ(COH)	1169–1260 (200)	913	Tyr or *p*-cresol, band sensitive to H-bonding for OH group, 256 cm^{-1} lower for O^{2}H group
Asp,Glu, ν(C − O)	1160–1253	1250–1300	Range in ^1H_2O from band position in aqueous solution near 1250 cm^{-1} [154,432] and shift observed for hydrogen bonded and free C^2H_3COOH [433]. Band position in ^2H_2O from isotope shifts of hydrogen bonded (data not shown) and free CH_3COOH [433]
His, ν(CN), δ(CH)	1104,1090,1106,1094	1104,1096,1107,1110	Values are for His^-, N1-, N3-protonated HisH and $HisH_2^+$, respectively
Trp, δ(CH), ν(NC)	1092		Indole infrared spectrum
Trp, ν(NC), δ(CH), ν(CC)	1064		Indole infrared spectrum
γ_t(CH_2)	1063–1295		Weak, couples with adjacent CH_2 groups, but in phase mode at 1300 cm^{-1} good group frequency [79]
Thr, ν(C − O)	1075–1150		2 bands expected
Ser, ν(C − O)	1030	1023	
Trp, ν(CC), δ(CH)	1012–1016	1012	
Ser, ν(CO) or ν(CC)	983		
Ser, ν(CO), δ(CO^{2}H)		940	
Thr, δ(CO^{2}H)		865–942	
γ_r(CH_2)	724–1174		Couples with adjacent CH_2 groups, in phase mode at 724 cm^{-1} most intense [79]

Extended and corrected version of a previous compilation [150].

If available, parameters of infrared spectra of amino acid side chains are given. If not, data are taken from infrared spectra of model compounds or from Raman spectra. Band positions are given for ^1H_2O and ^2H_2O, the latter are indicated by italic print. The shift upon $^1H/^2H$ exchange is given when a compound in both solvents is compared in the original work. The listing of internal coordinate contributions to a normal mode is according to their contribution to the potential energy of the normal mode (if specified in the literature): If the contribution of an internal coordinate to the potential energy of a normal vibration is ≥ 70% only that coordinate is listed. Two coordinates are listed if their contribution together is ≥ 70%. In all other cases those 3 coordinates that contribute strongest to the potential energy are listed. If no assignment is listed, no or multiple assignments are given in the original publications. Vibrations dominated by amide group motions are not included. ν stretching vibration, νs: symmetric stretching vibration, ν_{as}: antisymmetric stretching vibration, δ: in plane bending vibration, δ_{as}: asymmetric in plane bending vibration, γ_w: wagging vibration, γ_t: twisting vibration, γ_r: rocking vibration

References: aliphatic groups [79], Arg, Asn [152,154,155,424], Asp [152,154,155,432,433], Cys [434], Gln [152,154,155,435], Glu [154,155,432,433], His^- [65,426], HisH [65,154,426], $HisH_2^+$ [64,65,155], Lys [152,154,427], Phe [154], Pro [429,436,437], Ser [79,434,438,439], Thr [79,438], Trp, [162,430,440,441], Tyr [64,66,67,152,154,155,442,443].

ratio can be improved considerably by using infrared lasers [44,139–141,147,148] or by repeating the experiment many times [149].

7. The absorption of amino acid side chains

Amino acid side chains are often at the heart of the molecular mechanism of proteins. Thus, side chain absorption can provide very valuable information, in particular when it is possible to follow the fate of the participating groups in a single time-resolved experiment. The aim of this kind of research is to identify the catalytically important side chains and to deduce their environmental and structural changes from the spectrum in order to understand the molecular reaction mechanism. For example, information may be obtained on the protonation state, coordination of cations and hydrogen bonding.

Table 1 gives an overview of the infrared absorption of amino acid side chains in ^1H_2O and ^2H_2O [11,150], see also further compilations of infrared bands [4,151–156] and of Raman bands [157–162]. Only the strongest bands are listed in Table 1, or

those in a spectral window free of overlap by bands from other groups.

The absorption of a side chain in a protein may deviate significantly from its absorption in solution or in a crystal. The special environment provided by a protein is able to modulate strength and polarity of bonds, thus changing the vibrational frequency and the absorption coefficient. Therefore, the band positions given in the table should be regarded only as guidelines for the interpretation of spectra. It may be mentioned here that also the pK_a of acidic residues in proteins may differ significantly from solution values. An example is Asp-96 of bacteriorhodopsin for which a pK_a > 12 has been found [163].

8. The absorption of the protein backbone

8.1. Normal modes of the amide group

N-methylacetamide (NMA), shown in Fig. 3, is the smallest molecule that contains a *trans* peptide group. It has therefore become the starting point for a normal mode analysis of polypeptide backbone vibrations [151]. If the CH_3 groups are regarded as point masses, the number of atoms of NMA is 6 and thus there are 12 normal modes. Of these, the four highest frequency ones will be discussed in the following according to Krimm and Bandekar [151]. The contribution of internal coordinates to these normal modes will generally alter when the amide group is incorporated into a polypeptide.

8.1.1. NH stretching vibrations—amide A and B (~3300 and ~3070 cm^{-1})

The NH stretching vibration gives rise to the amide A band between 3310 and 3270 cm^{-1}. It is exclusively localised on the NH group and is therefore in proteins insensitive to the conformation of the polypeptide backbone. Its frequency depends on the strength of the hydrogen bond. The amide A band is usually part of a Fermi resonance doublet with the second component absorbing weakly between 3100 and 3030 cm^{-1} (amide B). In NMA and polypeptide helices, the NH stretching vibration is resonant with an overtone of the amide II vibration, in β-sheets with an amide II combination mode. An alternative assignment of the amide B band to the stretching vibration of intramolecularly hydrogen bonded NH groups has recently found experimental support [164].

8.1.2. Amide I (~1650 cm^{-1})

The amide I vibration, absorbing near 1650 cm^{-1}, arises mainly from the C═O stretching vibration with minor contributions from the out-of-phase CN stretching vibration, the CCN deformation and the NH in-plane bend. The latter is responsible for the sensitivity of the amide I band to N-deuteration of the backbone. In proteins, the extent to which the several internal coordinates contribute to the amide I normal mode depends on the backbone structure [151]. The amide I vibration is hardly affected by the nature of the side chain. It depends however on the secondary structure of the backbone and is therefore the amide vibration that is most commonly used for secondary structure analysis. The amide I band of proteins will be discussed in more detail below.

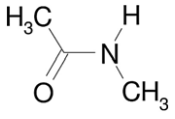

Fig. 3. Structure of *N*-methylacetamide (NMA). Reprinted with permission from [29]. © 2002 Cambridge University Press.

8.1.3. Amide II (~1550 cm^{-1})

The amide II mode is the out-of-phase combination of the NH in plane bend and the CN stretching vibration with smaller contributions from the CO in plane bend and the CC and NC stretching vibrations. Like for the amide I vibration, the amide II vibration of proteins is hardly affected by side chain vibrations but the correlation between protein secondary structure and frequency is less straightforward than for the amide I vibration. Nevertheless it provides valuable structural information and secondary structure prediction can be done with the amide II band alone [165].

N-deuteration converts the amide II mode to largely a CN stretching vibration at 1490–1460 cm^{-1} (named amide II′ mode). The N^2H bending vibration has a considerably lower frequency than the N^1H bending vibration and thus no longer couples with the CN stretching vibration. Instead, it mixes with other modes in the 1070–900 cm^{-1} region. Because NH bending contributes to the amide II mode but not to the amide II′ mode, both modes will be affected differently by backbone conformation and the environment of the amide group. For example, hydrogen bonding will be sensed predominantly by the NH bending vibration, which contributes to the amide II but not to the amide II′ vibration — the effect of a hydrogen bond will therefore be larger on the amide II vibration than on the amide II′ vibration. The internal coordinate contributions to the amide II vibration depend upon the backbone conformation with a trend to higher frequencies with increasing contribution of the NH bending vibration. The amide II band is weak or absent in the Raman spectrum [151].

8.1.4. Amide III (1400–1200 cm^{-1})

The amide III mode of NMA is the in-phase combination of the NH bending and the CN stretching vibration with small contributions from the CO in plane bending and the CC stretching vibration. In polypeptides, the composition of this mode is more complex, since it depends on side chain structure and since NH bending contributes to several modes in the 1400- to 1200-cm^{-1} region. In spite of side chain contributions to the amide III mode, this mode can be used for secondary structure prediction [166–169]. Upon N-deuteration, the N^2H bending vibration separates out and the other coordinates become redistributed into other modes.

8.2. The amide I vibration of proteins

The amide I band of polypeptides and proteins has long been known to be sensitive to secondary structure and this has caused

considerable interest into how structure relates to spectrum. However, explaining the large splitting of the amide I band of β-sheet structures has presented a challenge for theoreticians. Only with the introduction of the transition dipole coupling mechanism [170] this splitting in a main band near 1630 cm^{-1} and a side band near 1690 cm^{-1} could be explained. Other effects like through-bond coupling and hydrogen bonding also modify the amide I frequency of polypeptides to different degrees. In addition to these effects, which are discussed below, changing the dielectric constant of the environment from 1 to 80 (water) reduces the calculated frequency for NMA by 30 cm^{-1} [171] as suggested earlier for protein amide groups [172].

8.2.1. Transition dipole coupling (TDC)

The fundamental mechanism that renders the amide I vibration sensitive to secondary structure is transition dipole coupling (TDC) [170,173–177]. It is a resonance interaction between the oscillating dipoles of neighbouring amide groups and the coupling depends upon their relative orientation and their distance. Coupling is strongest when the coupled oscillators vibrate with the same frequency. TDC has two effects:

(i) *Exciton transfer*: if energy is absorbed by an oscillator it does not remain there but is rather transferred to a nearby oscillator with a typical time constant of 0.5 ps for an α-helix [178] — as a consequence the excited state is delocalised, typically over a length of 8 Å [178].
(ii) *Band splitting or exciton splitting*: TDC leads to a shift of the amide I frequency depending on the orientation, distance and relative phases of the coupled oscillators. If only two coupled oscillators are considered, two different excited energy levels are observed depending on whether the oscillators are in phase or out of phase. This phenomenon is called exciton splitting. The result is a splitting of the amide I band, which can be as large as ~70 cm^{-1} [179,180] for β-sheet structures.

The TDC formalism describes the oscillating charges in the dipole approximation. The background here is that any charge distribution can be represented by summing up a net charge, a net dipole, a net quadrupole and higher multipoles; if the electrostatic effects are observed far away from the location of the charges. In systems without net charge, like the amide group, the dipole contributes usually most and higher multipoles can be neglected. The dipole approximation of the TDC mechanism seems to provide a good description of the interactions between distant amide groups, i.e. those that are not nearest neighbours. At short distances (<6 Å [181]) the TDC approximation becomes less satisfactory [181–183]. The transition dipole moments of the individual amide I oscillators can be regarded as constant in a first approximation [112].

8.2.2. Through-bond coupling

Amide I and II vibrations involve small displacements of the C_α atom [151] which couples vibrations of the same kind in neighbouring peptide groups via the chemical bonds. There is evidence for some through-bond coupling between nearest neighbours from ab initio calculations on NMA [184] and di- and tripeptides [185–187] and from semiempirical calculations on larger peptides [188]. However, through-bond coupling does not seem to have a major effect on the amide I and II vibrations and cannot explain the large splitting of the amide I band of antiparallel β-sheet structures [170].

8.2.3. Hydrogen bonding

The effects of hydrogen bonding on the infrared spectrum of NMA have been examined computationally in ab initio calculations and experimentally [171,189–191]. Each of the two possible hydrogen bonds to the C═O group lowers the amide I frequency by 20 to 30 cm^{-1} and a hydrogen bond to the NH group by 10 to 20 cm^{-1} [171,190]. Further downshifts [190,191] and less frequency variation between different hydrogen bonding patterns [190] are obtained when a continuum model for water is included in the calculations. The combination of explicit water molecules in the first hydration shell and of a continuum model for water reproduces the experimentally observed shifts [190,191]. For polypeptides there is experimental evidence for an effect of hydrogen bonding on the amide I frequency since the different positions of the main absorption band at 1632 cm^{-1} for poly-β–L-Ala and at 1624 cm^{-1} for poly-β–L-Glu were tentatively explained by the stronger hydrogen bonds of the latter [151]. The side band of β-sheets at high wavenumbers however seems to be less affected by the strength of hydrogen bonding since it is observed within 1 cm^{-1} for the two polypeptides. For α-helices there is also evidence for an effect of hydrogen bonding on the vibrational frequency since solvated helices (i.e. helices forming hydrogen bonds also to solvent molecules) absorb approximately 20 cm^{-1} lower than non-solvated helices [40,192–195].

Much recent work has been done to model the effects of hydrogen bonding with electrostatic models as summarized recently [196]. The models differ as to whether the electric effects of the environment on a given amide group are accounted for by the electric potential [197–199], the electric field [200], or a combination of electric field and its derivatives [113,201]. These quantities are calculated at two [199] or four [113,198–200] atoms of the amide group, at six atoms of NMA [197,200], or at up to 65 sites of the amide group [201] and related to the amide I frequency via ab initio quantum chemical calculations. Several of the approaches have been compared and shown to yield similar results for NMA in water (^2H_2O) [200], but for the intramolecular interaction within small peptides, the correlation between frequency and electric potential works best [196].

8.2.4. Calculation of the amide I band

There are several ways of calculating the amide I band of a protein:

(i) For infinite secondary structures, their symmetry considerably reduces the number of observable vibrational modes and the effect of TDC is easily calculated. This simple approach can explain the general features of amide I absorbance of secondary structures [173–176,202].

(ii) For calculating the amide I band of proteins, a “floating oscillator model” has been developed [203,204]. The model

considers isolated amide I oscillators. The unperturbed oscillators vibrate with an intrinsic frequency ν_0. By adjusting the unperturbed frequency, effects of hydrogen bonding, non-planarity of the peptide group and through-bond interactions may be accounted for. A normal mode calculation is then carried out with a matrix of force constants that contains the diagonal force constants (which determine ν_0) and interaction force constants f_{AB} between amide group A and group B (which shift the frequency of the coupled vibration). The original model considered only interaction via TDC and had fixed intrinsic frequencies ν_0 for a given secondary structure type. It gave good agreement with some experimental protein spectra [203] whereas for the simulation of some other experimental protein spectra there is still room for improvement [205]. Nevertheless it has led to interesting insight [29,174–176,203,204,206] (see below). The extensive recent work outlined above has considerably increased our understanding of the factors that influence the amide I vibration. A more sophisticated floating oscillator model for proteins has already been presented [207] and other versions are under development. These have been outlined and tested against quantum chemical calculations of peptides [187,208,209]. In these amide I calculations, intrinsic frequency shifts and interaction force constants between nearest neighbours in sequence will be taken from density functional calculations and all other interactions will be calculated from TDC and models of hydrogen bonding.

(iii) A normal mode analysis can be carried out using a simplified general valence force field for the polypeptide with that of *N*-methylacetamide serving as a starting point [151]. The force field is then refined for a given polypeptide structure in order to match the calculated frequencies with the experiment. Hydrogen bonds can be included in the force field by assigning force constants to the H···O stretching and the N−H···O and C═O···H bending vibrations. TDC is also accounted for by interaction force constants f_{AB}, as described above for the floating oscillator approach. In contrast to the floating oscillator model for the amide I vibration, these calculations provide all vibrational frequencies of the polypeptide and were able to reproduce the observed vibrational spectra of regular polypeptides with an average error of 5 cm^{-1} [151]. Recently it was suggested that the transition dipole moment of a given amide group depends on coordinates of other groups. The implementation of this effect with interaction force constants from ab initio calculations of (L-Ala)$_2$ improved the calculated frequency of the E_2 mode considerably [210].

(iv) For small peptides with a defined structure, density functional calculations can be carried out that include transition dipole coupling, through-bond coupling and the effects of hydrogen bonds. [182,211,212]. The calculated force field and quantities like the derivative of the dipole moment μ can then be transferred to larger peptides.

8.3. How structure affects the amide I vibration — some rules of thumb

Computational and experimental studies have indicated a number of rules of thumb that describe how the amide I absorption depends on backbone structure. α-helices give rise to a main absorption band close to 1655 cm^{-1} and a shoulder at lower wavenumbers [174,203]. The band position of the main band shifts down with increasing helix length [174], when the helix is bent in coiled coils [192,213] and when the helix is solvent exposed (absorption maximum at 1640–1650 cm^{-1} in H_2O, at 1629–1640 cm^{-1} in ^2H_2O) [180,214–216]. Short α-helices with less than 6 residues do not always give rise to the typical α-helix absorption but can produce several bands throughout the amide I region [174,203].

Antiparallel β-sheets exhibit a strong band near 1630 cm^{-1} and a weaker band near 1685 cm^{-1}. The position of these bands is hardly affected by the number of amide groups in the strands of the sheet, but depends on the number of strands. Sheets with a larger number of strands have a lower spectral position of the main band [176,211]. Also the main band of parallel β-sheets shifts to lower wavenumbers with increasing number of strands [175]. Twisting of an antiparallel β-sheet causes its main band to shift to higher wavenumbers and reduces the splitting between high and low wavenumber band. The effect of twisting is less for parallel β-sheets [212]. Parallel β-sheets [173,175] have their main absorption at higher wavenumber than corresponding antiparallel β-sheets [173,176] although the difference can be as little as 4 cm^{-1} [217] and the parallel β-sheet band can be as low as 1622 cm^{-1} (in H_2O) for β-barrel proteins [218] and as low as 1619 cm^{-1} (in ^2H_2O) for peptides [217]. Parallel β-sheets exhibit a smaller splitting between their main and side band and their high wavenumber side band is less intense [175,176]. In consequence, the high-wavenumber side band is often, but not always, absent for parallel β-sheets [217–219]. The difference between parallel and antiparallel sheets becomes less pronounced when a parallel β-sheet with several strands is compared to an antiparallel sheet with few strands or which is twisted [175,176,212] which makes it experimentally difficult to distinguish between parallel and antiparallel sheets in proteins [203,218,220].

9. Overview of protein studies

9.1. Secondary structure

Probably the most common application of infrared spectroscopy in protein studies is the analysis of secondary structure [1,3,4,6,8–10,221,222]. Secondary structure analysis of proteins is nearly exclusively done using the amide I band, but the amide II [165] and amide III [166–169] bands as well as the near-infrared region [164,223–226] have also been shown to be useful. The importance of this infrared spectroscopic application might even increase in the proteomics age where vast numbers of proteins wait to be characterised. Anticipating this, work has started to develop a data bank in which protein spectra from different laboratories are to be collected [227].

Above it has been discussed that the sensitivity of the amide I band to the structure of the protein backbone is predominantly due to transition dipole coupling. The result is that a particular secondary structure absorbs predominantly in a specific range of

Table 2
Assignment of amide I band positions to secondary structure [29]

Secondary structure	Band position in ^1H_2O/cm^{-1}		Band position in ^2H_2O/cm^{-1}	
	Average	Extremes	Average	Extremes
α-helix	1654	1648–1657	1652	1642–1660
β-sheet	1633, 1684	1623–1641, 1674–1695	1630, 1679	1615–1638, 1672–1694
Turns	1672	1662–1686	1671	1653–1691
Disordered	1654	1642–1657	1645	1639–1654

The table is based on the experimental data and assignments of various authors collected and evaluated by Goormaghtigh et al. [6]. In similar tables a discrimination between parallel and antiparallel β-sheet can sometimes be found, because theory predicts no high wavenumber component for infinite parallel β-sheets [175]. However, as discussed above, similar spectra are expected for finite or twisted β-sheets [175,176,203,212] and there is no experimental evidence for a difference between the frequencies of parallel and antiparallel β-sheet [218,220].

the amide I region, as specified in Table 2. The two most common approaches to determine the secondary structure are: (i) fitting the amide I band with component bands [10,220,228] after identifying their position with band narrowing techniques [229–232] and (ii) decomposing the amide I band into basis spectra which have been calculated from a calibration set of spectra from proteins with known structure [10,233–238]. A neural network approach has also been applied [239]. Interestingly, a decent prediction of α-helix, β-sheet, β-turn and irregular structure content with errors in the prediction of ~7% and less is achieved using the absorption at only three wavenumbers (1545, 1611, and 1655 cm^{-1}) after careful pretreatment of the spectra. The error can be slightly reduced, and a prediction of the 3_{10}-helix content included, by using three, but not more, wavenumbers specifically for each secondary structure [240].

The sensitivity of the amide I vibration to secondary structure makes it possible to study protein folding, unfolding and aggregation with infrared spectroscopy. Representative examples are found in refs. [36–38,43,44,241–246] and the topic has been reviewed [7,43,244]. While the folded protein exhibits a structured amide I spectrum after band narrowing techniques have been applied, the unfolded protein shows a broad, featureless amide I band centred near 1650 cm^{-1} which is characteristic of unordered structure. In contrast, aggregated protein often shows a band near or below 1620 cm^{-1} which is characteristic of intermolecular β-sheets [7,247–249].

9.2. Flexibility

The amide II band is sensitive to $^1H/^2H$ exchange due to the contribution of the NH bending vibration to the amide II mode. $^1H/^2H$ exchange experiments probe the flexibility of proteins, since the exchange rate of the amide protons depends upon their solvent accessibility and the strength of their hydrogen bond [125,250,251]. A hydrogen bonded amide proton is protected from exchange even when it is exposed to the solvent. This has been shown for small molecules for which hydrogen bonding can slow down exchange rates by nearly six orders of magnitude [250]. Thus hydrogen bonds need to break by local or global unfolding for $^1H/^2H$ exchange to proceed at a significant rate. Peptide proton exchange is catalysed by OH^- down to pH 3 [250] which abstracts the peptide proton in a first step. Subsequently, the amide group will be deuterated by ^2H_2O.

$^1H/^2H$ exchange can be followed by monitoring the amide II band either in transmission or ATR experiments. In the former experiments, the protein is transferred to ^2H_2O, then placed in the infrared cuvette and recording of a series of time-resolved absorbance spectra started as soon as possible afterwards, typically within 15 min. With new mixing devices [36,117–119] these experiments can now be done with experimental dead times which are in the millisecond range and below. In ATR experiments, a dry protein film is prepared on the ATR crystal which has most of the free solvent water removed. Then nitrogen saturated with ^2H_2O is blown over the sample which starts $^1H/^2H$ exchange. During the first 2 min of the experiment, the film adjusts to the new conditions of humidity and swells which is limiting for the dead time of these experiments. In the evaluation of the time series of spectra, the contribution of side chain absorption to the amide II band has to be subtracted [252]. The exchange of most polar side chain protons is much faster than that of backbone protons because proton transfer to OH^- is energetically downhill for most side chains (pK_a of side chain $< pK_a$ of OH^-) [250] but not for peptide protons (pK_a of peptide $> pK_a$ of OH^-). Thus every encounter of an acidic side chain group with OH^- will abstract the side chain proton while on average 1000 collisions are needed to deprotonate an amide group [250]. As a consequence, side chain exchange is complete within 2 min for lysozyme at pH 8 [252]. The time course of the amide II band is typically fitted by three to four exponentials for amide groups with fast, medium and slow exchange. From this the percentage of amide groups that belong to each categories is obtained.

Exchange rates vary considerably between different proteins, from nearly complete exchange within 3 h for lactose permease [253] to more than 50% of peptide protons being exchange resistant for at least several hours for the K^+ channel of *Streptomyces lividans* [254], bacteriorhodopsin [255,256] and rhodopsin [255]. The exchange characteristics of proteins might depend on their particular physiological state and can be modulated by the binding of ligands [257,258], during catalysis [259] or by interaction with membranes [260].

In analysing different physiological states of a protein, $^1H/^2H$ exchange is an interesting complement to comparing the amide I absorption between the states. The latter quite often indicates that the net change of secondary structure is small, and this was found to be the case also for two ATPases upon ligand binding [257,258,261] whereas $^1H/^2H$ exchange of these proteins indicates that 10–20% of the residues alter their exchange characteristics. It emerges for these cases that the conformational change upon ligand binding involves a large number of residues as shown by the altered exchange characteristics but leads only to a small net change in secondary structure, either due to many compensating secondary structure changes, or due to movements of large domains with little impact on the secondary structure.

9.3. Function

Elucidating the molecular mechanism of proteins is a major challenge for the life science community. Infrared spectroscopy continues to provide important contributions in this field and combines several of its advantages in these studies: high time resolution (<1 μs), universal applicability from small soluble proteins to large membrane proteins and the high molecular information content combined with a sensitivity high enough to detect a change in the environment around a single atom of a large protein.

In favourable cases, effects of a protein reaction on the infrared spectrum can already be observed in the absorbance spectrum [99,249,262,263]. In other cases, the associated infrared absorbance changes have to be monitored; or in other words: the associated infrared difference spectrum has to be recorded. This has been done by carefully subtracting the spectrum of a sample where the protein is in state B from a spectrum where it is in state A [262,264–271]. However, the absorbance changes usually observed for protein reactions are very small, on the order of 0.1% of the maximum absorbance. In consequence, the approach described above does not generally allow the sensitive detection of the small absorbance changes between the two protein states. Instead, the protein reaction of interest has to be initiated directly in the cuvette. This technique is termed *reaction-induced infrared difference spectroscopy*. It will be described in detail in Sections 10–12 and has been reviewed before [2,12–20,23–33,272]. There are a number of reviews focusing on Raman spectroscopy of enzyme reactions of ligand–protein interactions [53–56,59,61] that are well worth reading also for the infrared spectroscopist.

9.4. Enzyme activity measurements with infrared spectroscopy

Enzyme activity is the basis of many biotechnological processes. It is usually measured indirectly because substrate and product cannot be distinguished in the UV or visible range of the spectrum. Therefore coloured or fluorescent substrate analogues have been developed or the enzymatic reaction of interest is coupled to auxiliary enzymatic reactions that can be followed in the UV or visible spectral range. In contrast, infrared spectroscopy can provide a direct, "on-line" monitor of enzymatic reactions, because the infrared spectra of educts and products of an enzymatic reaction are often different. Examples for infrared spectroscopic measurements of enzyme activity are cefoxitin hydrolysis by β-lactamase [77], deacylation of cinnamoyl-chymotrypsin [78], ATP hydrolysis by the Ca^{2+}-ATPase [72], oxidation of D-glucose by glucose oxidase [74], hydrolysis of amides [76,273], synthesis of hydroxamic acid derivatives [273] by amidase and the reaction of α-ketoglutarate and Ala to Glu and pyruvate by glutamic-pyruvic transaminase [153].

9.5. Water and hydrated protons in proteins

Water is not only as solvent essential for protein structure, it is often also intimately linked to protein function, for example when it participates in biochemical reactions as solvent or reactant, or when it constitutes proton pathways to and from active sites in proteins. No attempt is made here to review the vast literature on infrared spectroscopy of water and water's interaction with proteins, only selected examples are given. Infrared spectroscopy of liquid water [274–276] and water clusters [277] has been reviewed recently. Molar absorptivities of the absorption bands of liquid water can be found in ref. [120].

Hydration of proteins has been studied by infrared spectroscopy as reviewed previously [276,278]. Hydration of lysozyme [278,279] and bovine serum albumin [280] involves (i) protonation of carboxylate groups, (ii) formation of hydrogen bonds between water and the C═O and N−H groups of the protein backbone, some of which replace direct N−H···O═C hydrogen bonds, and (iii) insertion of water without affecting protein hydrogen bonds. A considerable number of water molecules remains associated with the dried proteins. Nevertheless, approximately a quarter of all N−H and C═O groups are not hydrogen bonded when the proteins are dry. In hydrated lysozyme, about 50% of the N−H and C═O groups are hydrogen bonded to water [279].

Individual protein-bound water molecules can also be observed directly with reaction-induced infrared difference spectroscopy (see Section 10). Here the relatively strong absorption of water, which is usually regarded as a problem, turns into an advantage. In the spectral region of water's bending vibration near 1640 cm^{-1} it has been detected that the oxidation of the primary donor of the bacterial photosynthetic reaction of *Rhodobacter sphaeroides* centre affects water molecule(s) [281].

In protein films with little free water, even the region of the stretching vibration of water can be analyzed (~3400 cm^{-1} in ^1H_2O and 2500 cm^{-1} in ^2H_2O). The absorption of water molecules is identified with help of the small isotope shift upon $^{16}O \rightarrow {}^{18}O$ substitution and localised in the protein by mutating putatively interacting amino acids. These experiments provide spatially resolved information about functionally important water molecules, for example in bacteriorhodopsin [16,282–287], rhodopsin [16,283,288], sensory rhodopsin [289], photosystem II [290] and cytochrome *c* oxidase [291]. These water molecules can be detected because they experience a change in hydrogen bonding. The symmetric and antisymmetric stretching vibrations of non-hydrogen bonded water absorb between 3630 and 3760 cm^{-1} [274,277,292–296], whereas bonded OH groups absorb between 3600 and 2900 cm^{-1} depending on the strength and pattern of hydrogen bonding [274,277,295].

Protonated water clusters give rise to a particular absorption spectrum that depends critically on the number of water molecules over which the proton is delocalised [297]. In particular, the isolated (i.e. non-solvated) Eigen cation $H_3O^+(H_2O)_3$ has a characteristic absorption at 2665 cm^{-1} (OH stretch) [297,298] and the isolated Zundel cation $H_2O{\cdots}H^+{\cdots}OH_2$ near 1750 cm^{-1} (HOH bend) and 1050 cm^{-1} ($O{\cdots}H^+{\cdots}O$ stretch or bend) [297,299]. An acidic aqueous solution exhibits a broad continuous absorption between 1000 and 3100 cm^{-1} and additional bands with respect to neutral water near 1200, 1740, and 2900 cm^{-1} [269,300–303] consistent with the presence of both, the Eigen and the Zundel forms of the hydrated proton [303].

Infrared spectroscopy has detected protonated water clusters in proteins, for example in a bacterial reaction centre [302] and in bacteriorhodopsin [304–307], where the localisation of the proton is affected by mutation of nearby amino acids [307]. The absorption is consistent with an Eigen cation in the former case and with Zundel and Eigen cations [307,308] in the latter.

10. Studying protein function with reaction-induced infrared difference spectroscopy

10.1. Principles

As mentioned before, the many overlapping bands in the absorption spectrum of proteins limit the information that can be obtained from an absorption spectrum. The key to obtain detailed structural information is to reduce the number of groups that contribute to a spectrum. This can be done by difference techniques. They are particularly suited to investigate the molecular basis of a protein reaction. Thus the infrared absorbance changes associated with the reaction are monitored; or in other words, the associated infrared difference spectrum is recorded. The absorbance changes usually observed for protein reactions are very small, on the order of 0.1% of the maximum absorbance. In consequence, simply comparing the spectrum of a sample where the protein is in state A with a spectrum where it is in state B does usually not allow the sensitive detection of the small absorbance changes between the two protein states. Instead, the protein reaction of interest has to be initiated directly in the cuvette and the associated infrared absorbance changes can be recorded [2,10,20,23,135].

10.2. Ways to trigger protein reactions

The number of methods to initiate protein reactions has constantly increased in the last decade. They have been reviewed before [2,14,15,18,20,24,25,27,28,30] and are only briefly discussed here.

Light-induced infrared difference spectroscopy has been the first technique that has been applied to proteins from the early 1980s. Here, continuous illumination or a light flash induces a reaction in photosensitive proteins like bacteriorhodopsin [14–17] or photosynthetic reaction centers [12,13,21,22]. From spectra recorded before and during/after illumination, light-induced difference spectra can be calculated.

Concentration jump techniques are required to study the effects of ions or molecules on proteins. Three different approaches have been applied to generate a concentration jump in an infrared sample: (i) the ATR technique, (ii) the infrared variants of the stopped-flow and continuous-flow techniques, and (iii) the photolytical release of effector substances from biologically "silent" precursors (termed "caged compounds").

Attenuated total reflection has the advantage that manipulation of medium composition is straightforward when a stable protein film can be prepared. For example ligands can be added or the pH can be changed. Examples are studies of ligand binding to the nicotinic acetylcholine receptor [309,310], to the gastric H^+/K^+-ATPase [261], to transhydrogenase [116], and of protein–protein interaction between transducin and rhodopsin [129].

Rapid mixing techniques are difficult to apply in infrared spectroscopy because of the viscous consistency of a concentrated protein solution and the small pathlength of less than 10 μm for measurements in ^1H_2O. Nevertheless, successful applications of mixing devices have been reported, as reviewed recently [244], first with the larger pathlength of 50 μm for ^2H_2O [118] and subsequently with 20 μm [117] and around 10 μm for ^1H_2O [36,119].

A *photolytically induced concentration jump* can be achieved with photosensitive molecules that release a compound of interest upon illumination in the UV spectral range (300–350 nm). These molecules are termed caged compounds and have been used for 30 years to study biological reactions [311–317]. In its caged form, the effector compound is modified such that it does not react with the protein of interest (see Fig. 4 for caged ATP). Photolysis of the caged compound leads to a sudden concentration jump of the free effector substance (<10 ms for caged ATP of Fig. 4, other compounds are faster). Binding of the effector substance to a protein and subsequent conformational changes alter the infrared spectrum. In addition to protein and

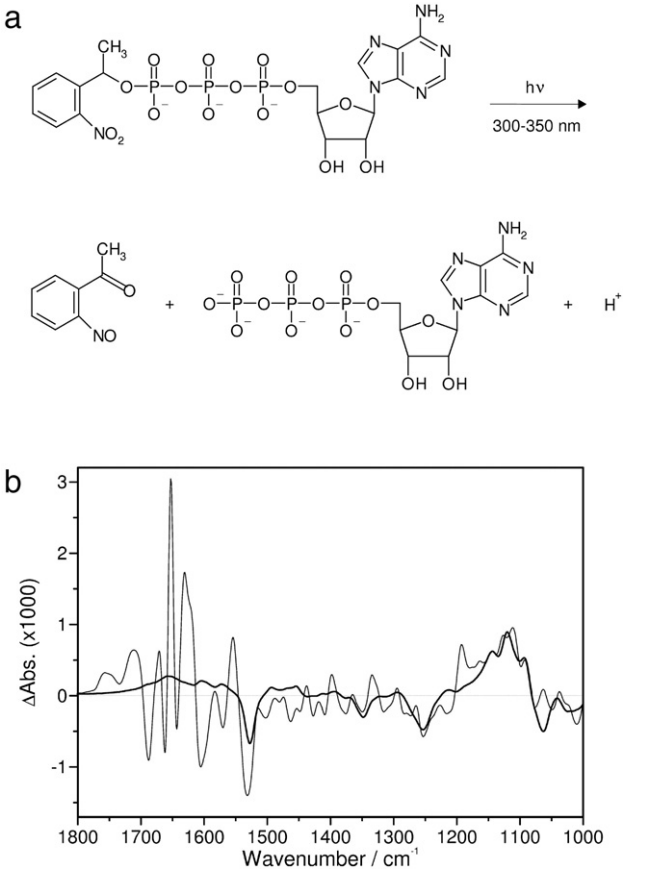

Fig. 4. Caged ATP. (a) Photolysis of caged ATP (b) Infrared difference spectrum upon release of ATP from caged ATP. Thick line: spectrum of caged ATP photolysis in the absence of protein. Thin line: ATP release in a Ca^{2+} ATPase sample. Two reactions contribute to the signals: (i) caged ATP photolysis and (ii) the transition of the Ca^{2+} bound ATPase to the E2P phosphoenzyme where Ca^{2+} has been pumped and released [349]. Reprinted with permission from [30]. © 2002 American Chemical Society.

effector molecule bands, the photolysis reaction is reflected in the difference spectra. In infrared studies of proteins, caged nucleotides, caged Ca^{2+} (Nitr-5 or DM-Nitrophen) and "caged electrons" (described in the photoreduction section) have been used most often. The studies undertaken have dealt with two main aspects, molecule–protein recognition and the molecular basis of enzyme function. Most of these studies have been done on the sarcoplasmic reticulum Ca^{2+}-ATPase, which has also been the first enzyme to be studied with this technique [318]. Further information can be found in refs. [19,31,319–322]. A recent extension of the approach uses helper enzymes to induce further reactions after the primary concentration jump and has been used to study ADP dissociation from the phosphorylated Ca^{2+}-ATPase after phosphorylation had been induced by ATP release from caged ATP [323].

Temperature- and pressure-jumps can be used to study folding and unfolding of proteins. The temperature jump is generated either by injecting a protein solution into a cuvette that is held at a different temperature (time resolution 100 ms) [241,243], by a laser pulse near 2 μm that is absorbed by the sample solvent ^2H_2O [40,43,324,325] (temperature maximum reached after 20 ns [43]) or by a visible laser pulse that excites a heat transducing dye [326,327]. Pressure-jump experiments [328,329] require a cell that allows to set the sample under pressures of several kbar and have an experimental dead time of about 20 s.

Equilibrium electrochemistry can be used to initiate redox reactions of proteins. Infrared investigations became available with the development of an ultra-thin-layer spectroelectrochemical cell suitable for protein investigations in aqueous solution [330]. The spectroelectrochemical cell permits control of the redox state of proteins in the infrared cuvette by applying a potential to a working electrode which changes the potential of the sample volume that is probed by the infrared beam. By applying a potential step at the working electrode, a redox reaction can be triggered in the electrochemical cell. From the infrared absorbance spectrum before and after the potential step, a difference spectrum can be calculated that reflects only the redox reaction of the protein.

The electrochemical cell is particularly useful when a protein contains several redox active cofactors with different midpoint potentials as it is often the case for proteins involved in photosynthesis and respiration. Since the method allows the accurate control of the sample redox state, it is possible to selectively induce the redox reaction of only one particular cofactor, i.e. to "dial-a-cofactor" [28]. Selective triggering of only one of the possible redox reactions has been achieved for example in studies on the charge separation catalysed by the bacterial photosynthetic reaction center. It was possible to separate the reaction of the primary electron donor (bacteriochlorophyll dimer) [281] from that of the electron acceptors quinone A or B [331]. In a study of photosystem I, careful experimentation avoided the oxidation of the abundant antenna chlorophylls and allowed the exclusive titration of signals of the primary electron donor P700 (a chlorophyll dimer) [332]. And as a final example, it could be shown that Glu^{278} of the *Paracoccus denitrificans* cytochrome *c* oxidase is involved in the redox reaction of heme *a* (and possibly Cu_B) [333]. More information on this method can be found in reviews [12,21,30,32]. While much of the initial work has been on photosynthetic proteins (see references above), recent work has concentrated on cytochrome *c* oxidases [32,333–340].

Photoreduction is a second way to induce redox reactions. It is based on photoexcitable electron donors like riboflavin [341,342] or Ru^{2+} complexes [343] for which the expression "caged electron" has been coined [344]. Light absorption converts these systems directly or indirectly to a highly reducing state which can transfer one electron to a protein. The principle is similar to that of photosynthetic reaction centers where photoexcitation of the primary donor produces a highly reducing excited state and initiates electron transfer reactions within the protein. Photoreduction has been used in studies of aa_3 cytochrome *c* oxidase of *R. sphaeroides* [344], bo_3 [344–346] and *bd* [347] ubiquinol oxidases of *Escherichia coli* and cytochrome $P\text{-}450_{cam}$ [343].

11. Interpretation of difference spectra

11.1. The origin of difference bands

Bands appear in difference spectra of protein reactions for several reasons: the chemical structure might change (protonation of carboxyl groups, catalytic reactions) or the three-dimensional structure of protein or cofactor. The former gives rise to a different absorption pattern before and after the reaction. The latter changes vibrational coupling between neighbouring groups or the environment around particular functional groups causing band shifts and changes in absorption index. In many cases, negative bands in a difference spectrum are characteristic of the state before the reaction and positive bands with that after the reaction. This interpretation might be misleading in the case of a change in absorption index since only the strength of absorption is affected but not the band position.

11.2. The difference spectrum seen as a fingerprint of conformational change

It is often difficult to extract the wealth of information from a difference spectrum. A simple approach is to regard the spectra as a characteristic fingerprint of the conformational change. The signature of a conformational change in the spectrum can then be used to detect and define transient conformational states of a protein. Similar approaches have a long tradition in fluorescence and absorption spectroscopy. The approach can be used to study reaction intermediates and to classify and quantify conformational changes. It has even provided molecular information in a study that mapped substrate protein interactions [348].

11.2.1. Intermediates

From the time course it is possible to evaluate the number of intermediates in the reaction. Here, time-resolved vibrational spectroscopy has the advantage that the observation is not restricted to a limited number of chromophores (i.e. Trp residues) or to an extrinsic fluorescence label which will largely

reflect local changes in the vicinity of the chromophore(s) and may miss conformational changes occurring in distant regions of the protein. Instead, in vibrational spectroscopy all carbonyl "chromophores" of the backbone amide groups are monitored, and this will reveal any change in backbone conformation even if very small. In the same experiment it is possible to follow additionally the fate of individually catalytically "acting" groups. Thus, infrared spectroscopy simultaneously looks, on the one hand locally at the catalytic site, and on the other hand at the protein as a whole. This approach has been used in studies of the Ca^{2+}-ATPase pump mechanism [349] of the photoactive yellow protein photocycle [350], and of protein folding studies [36,38,42,43].

11.2.2. Similar conformational changes

From the shape of the spectra, conformational changes can be classified according to their similarity. This can be used to compare different preparations of a protein or related partial reactions [62,309,332,336].

11.2.3. The extent of conformational change

From the magnitude of the difference signals, the extent of conformational change in a protein reaction may be estimated using the amide I region of the spectrum [257,349,351,352]. While this approach has several implications and limitations, as discussed previously [11,29,349], it nevertheless seems to provide realistic estimates of the *net* secondary structure change [11,29,353].

11.3. Molecular interpretation: Band assignment

Infrared difference spectra usually contain many difference bands which indicate the wealth of information that is encoded in the spectrum. However, extracting this information is often difficult and ideally requires the assignment of the difference signals to individual molecular groups of the protein. Assignment of infrared bands to specific chemical bonds is possible by studying model compounds, by chemical modifications of cofactors or ligands, by site-directed mutagenesis and by isotopic labeling of ligands, cofactors and amino acids.

Model spectra. contributions of cofactors or substrate molecules to the infrared spectrum can be identified by normal mode calculations or by comparison with the spectra of the isolated molecules or model compounds in an appropriate environment. An example are chlorophyll studies [354–356].

Site-directed mutagenesis is a very powerful approach. Ideally, an infrared signal due to a specific amino acid is missing when this amino acid has been selectively replaced. The missing signal can then be assigned to the mutated amino acid. Examples for this assignment strategy can be found in Section 12. However, mutagenesis cannot be applied to crucial amino acids because their mutation abolishes protein function. Also, a mutation may exert wide-spread conformational effects on the protein which extensively modify the structural changes and thus the infrared difference spectrum. Therefore, the effect of mutation on infrared difference spectra has to be evaluated very carefully.

Isotopic labeling has been used as a powerful tool since the early days of infrared spectroscopy on proteins, in order to observe a specific group in a large protein [264,266]. It avoids perturbations of protein structure that might be introduced by mutagenesis and allows to label crucial amino acids that cannot be mutated without loss of function. Due to the mass effect on vibrational frequencies, infrared absorption bands of a labeled group are shifted with respect to those of the unlabeled groups and can be identified in the spectrum. Ligands, cofactors and protein side chains as well as backbone groups can be labeled.

Labeling ligands is very informative when the interactions between ligands and proteins are investigated, as illustrated by studies on the binding of CO [264] and O_2 [357] to hemoglobin, of O_2 [357] to myoglobin, of carbonyl groups to triosephosphate isomerase [266] and phospholipase A_2 [358], and of phosphate groups to Ras [91,114,359,360] and Ca^{2+}-ATPase [361]. Protein cofactors have also been labeled for example for bacteriorhodopsin [17,362], photosynthetic reaction centres [12,13,22] and cytochrome *c* oxidase [335].

In favourable cases the substrate can transfer a labeled group to the protein which can then be studied in its protein environment. This approach has been used to study the acyl enzyme of serine proteases [27,78,268] and the phosphate group of the phosphoenzyme intermediates of the Ca^{2+}-ATPase [69,70,93,361].

Amino acids in proteins can be labeled in various ways. $^1H/^2H$ exchange is simply done by replacing ^1H_2O by ^2H_2O which exchanges the protons of accessible acidic groups, like OH, NH and SH groups, by deuteriums [250]. The observed characteristic band shifts often allow the assignment of these bands to peptide groups or to specific amino acid side chains. An additional advantage is the shift of the strong water absorbance away from the amide I region (1610–1700 cm^{-1}) which is sensitive to protein structure. Recombinant proteins can be labeled uniformly with for example ^{13}C or ^{15}N [363], all amino acids of one type can be labeled, or a label can be placed specifically on one particular amino acid [364,365]. This site-directed labeling is the most powerful interpretation tool, unfortunately, it requires great effort and is usually not feasible.

The labeling of backbone carbonyls with ^{13}C shifts the amide I band by 36–38 cm^{-1} to lower wavenumbers [363,366–368]. This can be used to separate the amide I bands of two proteins or a protein and a peptide for binding studies [369,370], to probe the local secondary structure of peptides [188,211,371–375] or to determine band shifts due to hydrogen bonding to water [194,195].

11.4. Molecular interpretation: quantification

Once a band is assigned to a specific vibration, this is evidence that the assigned group participates in the studied protein reaction. Furthermore its frequency or the wavenumber of the corresponding infrared band provides precise information on a number of bond parameters and other molecular properties [84]. The quantitative interpretation becomes even more powerful with the increased ease of quantum chemical calculations of the vibrational spectrum as applied for example

to NMA (see Section 8.2). For enzymes, the information obtained from calculations is a telltale of how the environment shapes the molecular properties of catalytically active groups and some examples have been given in Section 3. This is the information needed to unveil the secrets behind the amazing catalytic power of enzymes.

12. Reaction-induced infrared difference spectroscopy—selected examples

12.1. Introduction

In the following, reaction-induced infrared difference spectroscopy is illustrated at the example of three different proteins. All three pump ions, driven either by light, redox potential or ATP. The biological systems required different adaptations of the difference principle to the biological system: bacteriorhodopsin highlights light-induced difference spectroscopy, cytochrome *c* oxidase has been studied with a variety of techniques and the Ca^{2+}-ATPase has been triggered by photolytically induced concentration jumps.

12.2. Bacteriorhodopsin

Bacteriorhodopsin is a light-driven proton pump of *Haloarchea* which serves as emergency energy source when the oxygen supply is low. Light is absorbed by the chromophore retinal that is covalently linked via a Schiff base to Lys-216. Light absorption in the light-adapted state causes isomerization of retinal from all-*trans* to 13-*cis*. The strained photoisomerized state of the protein relaxes back to its ground state in a series of reaction steps that are accompanied by proton transfer from the intracellular side to the extracellular side of the plasma membrane. The photocycle intermediates are named with letters J to O and can be followed by visible spectroscopy because of changes in retinal absorption.

Bacteriorhodopsin was one of the first proteins studied with reaction-induced infrared difference spectroscopy [376] since its photocycle can be conveniently triggered by light. The robustness of bacteriorhodopsin made it possible to apply time-resolved techniques like single wavelength measurements with a global source [377–379], stroboscopic FTIR spectroscopy [380,381] and the step scan technique [144,382,383] which require numerous repetitions of the flash-induced experiment on a single sample. A time resolution in the sub-microsecond range and trapping of intermediates at low temperature enabled characterisation of the structural changes upon proton pumping. Of particular importance was the identification of the proton transporting groups from the early detection of protonated carboxyl groups [376,378] to the assignment to specific residues or a localised protonated water cluster using isotopic labeling [384–386] and site-directed mutagenesis [307,385–388]. Combining this knowledge from infrared spectroscopy with that from recent structures at atomic resolution "the path of the proton through the membrane can now be followed in exquisite detail" [389]. Up to now all major intermediates have been crystallized, but infrared spectroscopy continues to deliver important insights because "…FTIR spectroscopy is a more sensitive method to detect small structural perturbations than crystallography at the available resolutions" [390]. As discussed in Section 3.4, infrared spectroscopy detects bond length changes in the picometer range.

Infrared spectroscopy on bacteriorhodopsin has been reviewed before [15–17,23,34,35]. In the following I will mainly discuss the contributions of infrared spectroscopy to identifying the proton transfer steps. Other important contributions have characterised the conformation of the retinal [362,391,392] to be a twisted 13-*cis* conformation in the early K intermediate that relaxes to the final *cis* conformation in the transitions to the KL and L intermediates [379,382,393]. Current research deals with the transmission of conformational changes through the protein [394], active water molecules [282,287] and protonated water clusters [304–306,395].

The retinal Schiff base remains protonated in the early phase of the photocycle [391]. Its proton is transferred to Asp-85 upon formation of the M intermediate [380,385,387,396] as identified by mutation of this residue [385,387]. To make this happen, the pK_a value of Asp-85 dramatically increases to more than 10.5 in the late M intermediate (M_2) [397] because of a drop in the effective dielectric constant to a value of 2 which was concluded from the spectral position of the Asp-85 C═O band [397]. Proton transfer to Asp-85 is accompanied by proton release to the extracellular side from a protonated water cluster close to Glu-194 and Glu-204 [307]. Interestingly, proton release is from residue 204 when this residue or Glu-194 are mutated to Asp [307].

Asp-96, located towards the cytoplasmic side from the Schiff base, is protonated in the early phase of the photocycle. Its signature can be detected because it experiences an environmental change upon formation of the L intermediate that was assigned with help of site-directed mutagenesis [386–388]. Upon formation of the N intermediate it becomes deprotonated [380,386,398] as the Schiff base reprotonates [396]. Asp-96 has an unusually high pK_a value >11 in the bacteriorhodopsin ground state [163,399] that decreases [398] to 7.1 in the N intermediate [163]. This pK_a change causes deprotonation of Asp-96 independent of the protonation state of the Schiff base [398]. Following reprotonation of Asp-96 from the cytoplasm, the final proton movement in the photocycle is from Asp-85 likely via Asp-212 [400,401] to the extracellular release site.

12.3. Cytochrome c oxidase and related heme-copper oxidases

Cytochrome *c* oxidase is the terminal electron acceptor in the respiratory chain and reduces an oxygen molecule to water. The reaction needs the input of four electrons from cytochrome *c* and four protons from the mitochondrial matrix or bacterial cytoplasm. In addition, four protons are pumped from matrix to intermembrane space in mitochondria or from cytoplasm to periplasm in bacteria. The enzyme contains four redox-active metal centres: Cu_A, heme *a*, heme a_3 and Cu_B. The latter two constitute the catalytic centre where the reduction of oxygen takes place.

Cytochrome *c* oxidases and related heme-copper oxidases have been studied with a variety of infrared spectroscopic techniques as reviewed previously [32] including photodissociation of carbon monoxide (CO) [402], electrochemistry [334], photoreduction [345] and ATR spectroscopy [403,404]. In the following, selected examples will be discussed.

Work on CO photodissociation is facilitated by the high wavenumber of CO absorption above 1900 cm^{-1} which puts it in a spectral window without overlapping absorption from other protein components. CO binds to heme a_3 in the dark, dissociates upon illumination and binds to Cu_B at low temperatures. At room temperature it can leave the enzyme upon photodissociation and appear in the bulk solution. Already in 1981, CO photodissociation experiments have led to significant conclusions regarding the catalytic centre [402]. Multiple CO absorption bands when bound to both metal centres indicated structural heterogeneity. From the different band widths it was concluded that the CO complex with Cu_B is more flexible than that with heme a_3 and experiences a nonpolar environment in the latter. Most importantly, the movement of CO between the two metal centres suggested that they line a cavity to which oxygen can bind and even the prediction of the distance between them turned out to be correct. These experiments were done below 100 K; that CO binds to Cu_B also at room temperature has been detected in one of the early applications of time-resolved single wavelength spectroscopy with tunable infrared laser diodes [147]. Combining CO photodissociation with site-directed mutagenesis [405] has excluded His-284 (cytochrome bo_3 from *E. coli*) as ligand of heme a_3 because the bands of the CO complex with heme a_3 were not affected by mutation of this residue. In contrast, bands of the complex with Cu_B were affected, in line with His-284 ligating Cu_B.

As cytochrome *c* oxidase translocates protons, much work has been devoted to identify the protonation sites. Protonated Glu-278 (*P. denitrificans*), at the end of one of the proton pathways to the catalytic centre, is involved in electron transfer reactions [333,338] as shown by site-directed mutagenesis in combination with infrared spectroscopy. The same holds for the corresponding residue Glu-286 in cytochrome bo_3 from *E. coli* [345]. A pH series has revealed that the equilibrium pK_a of Glu-278 in the *P. denitrificans* oxidase is larger than 10 in the reduced and oxidized states [291]. The corresponding Glu-286 in *Rhodobacter spaeroides* oxidase undergoes protonation changes during catalysis [406], indicating that its pK_a is modulated by a changing protein environment.

Further evidence for the participation of protonated carboxyl groups has been obtained for heme propionates from isotopic labeling [335]. Additional site-directed mutagenesis experiments have suggested that it is the ring D propionate of heme *a* that accepts a proton upon reduction of the enzyme [339]. In experiments that have exploited the natural sequence variety, it has been found that oxidation of bovine heart cytochrome *c* oxidase produces signals in the difference spectrum that are not observed for the oxidase of *P. denitrificans*. This has indicated protonation of a carboxyl group upon oxidation of bovine heart oxidase, possibly that of Asp-51, which is not conserved between the two enzymes [337]. The results are in line with the proposed role of this residue in proton pumping by mammalian oxidases [407]. A further protonation of a carboxyl group – Asp-75 – has been detected upon reduction of ubiquinone bound to *E. coli* cytochrome bo_3 [408], which is consistent with Asp-75 being located near the quinone binding site.

Evidence for Tyr protonation changes has also been obtained [406] and tentatively assigned to the unusual, covalently linked His and Tyr residues close to Cu_B. The signature of this moiety in infrared spectra has been identified by combining isotopic labeling of Tyr with site-directed mutagenesis [409], and by combining isotopic labeling of Tyr and of His [410–412]. The linked residues undergo significant changes during catalysis. While the protonation state of the Tyr moiety is not finally settled, the experiments favour a deprotonated Tyr in the oxidized state [411]. Labeling of Tyr and His residues has also revealed that their backbone carbonyls contribute significantly in the amide I region presumably due to a conformational change of the His-276 to Tyr-280 loop [411].

A band of a non-hydrogen bonded water hydroxyl appears upon reduction of the enzyme [291]. This assignment has been obtained by comparing experiments in H_2O, ^2H_2O and $H_2^{18}O$. The prospect is exciting that this band might originate from the water molecule that is produced in the catalytic reaction.

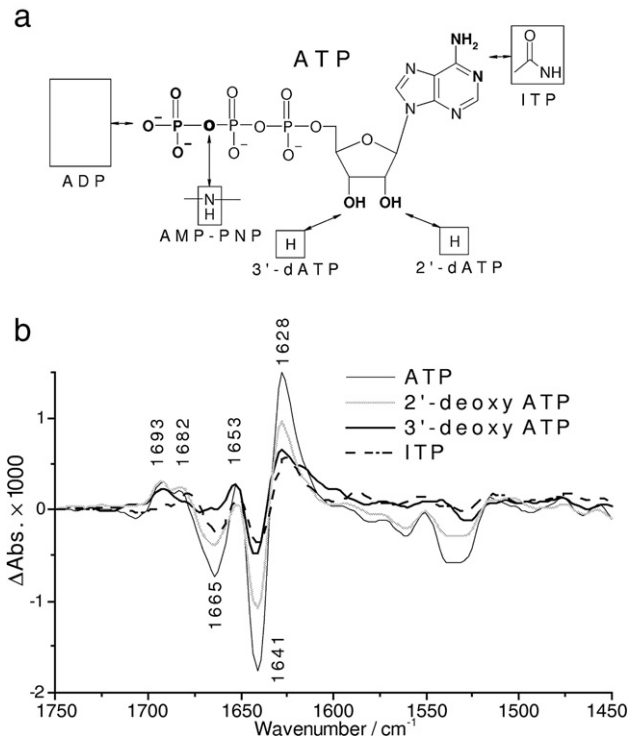

Fig. 5. (a) Structures of ATP and ATP analogues highlighting the modified functional groups of ATP. (b) Difference spectra of nucleotide binding to the Ca^{2+} ATPase ($Ca_2E1 \rightarrow Ca_2E1NTP$) obtained with ATP, 2′ deoxyATP, 3′ deoxyATP and ITP (1 °C and pH 7.5) [348]. Labels indicate the band positions of the ATP binding spectrum. The spectra show that the modification of each functional group of ATP affects the binding induced conformational change. Thus all these groups are involved in important interactions with the ATPase. Reprinted from [11]. © 2006 Nova Science Publishers.

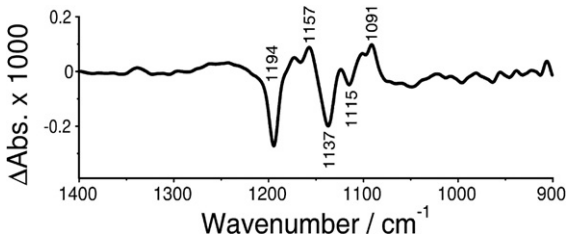

Fig. 6. Infrared difference spectrum of E2 $P^{16}O_3 \rightarrow$ E2 $P^{18}O_3$ isotope exchange at the phosphate group [93]. Spectra of isotope exchange were calculated by subtracting the spectrum before exchange from the spectrum after exchange. Reprinted from [11]. © 2006 Nova Science Publishers.

12.4. Ca^{2+}-ATPase

The Ca^{2+}-ATPase belongs to the family of P-type ATPases which are major players in active transport across biological membranes. It couples the pumping of two Ca^{2+} to the hydrolysis of one ATP molecule. It was the first protein to be studied by a photolytically induced concentration jump [318]. Caged ATP [71,318,349,413] and caged Ca^{2+} [352,414,415] have been predominantly used. The rapid scan technique with a time resolution of 65 ms is sufficient to kinetically resolve the main intermediates in the pump cycle after ATP release [349].

12.4.1. Nucleotide binding

One line of studies has been to map interactions between protein and substrate ATP. Fig. 5 shows infrared absorbance changes induced by nucleotide binding to the Ca^{2+}-ATPase. The spectra reveal the difference in absorbance between the initial nucleotide-free state Ca_2E1 and the nucleotide-ATPase complex Ca_2E1NTP.

The difference spectra reflect conformational changes of the protein backbone in the amide I (1700–1610 cm^{-1}) region of the spectra: the positive signal near 1653 cm^{-1} is characteristic of α-helical structure, the signals near 1693, 1641 and 1628 cm^{-1} of β-sheets. Turn structures likely contribute to the signals near 1665 cm^{-1}. The spectrum indicates that α-helices, β-sheets and turns are affected by ATP binding.

The nucleotide binding spectra are different for different nucleotides with the largest bands observed for ATP. Therefore, the conformational change upon nucleotide binding depends to a surprising degree on individual interactions between ATPase and nucleotide [348,416]. It has been concluded that the ATPase interacts with the γ-phosphate [416], the ribose hydroxyls and the amino function [348] of ATP. This has later been confirmed by X-ray crystallography [417,418]. The missing of individual interactions produces more than just local effects: it affects the entire conformational change upon binding. This suggests a concerted conformational change for which all interactions need to be in place [348].

Transfer of the nucleotidic γ-phosphate to Asp^{351} follows nucleotide binding. In this reaction, an interesting feature has been observed with ITP: the phosphorylation spectrum obtained with ITP shows additional signals in the amide I region as compared to ATP, which are similar to nucleotide binding signals [353]. Thus it seems that upon phosphorylation with ITP the enzyme catches up on a conformational change that cannot be achieved by ITP binding because the interactions between protein and base moiety are impaired.

The phosphorylation rate also depends on the type of nucleotide [353]. Upon dissociation of ADP from the phosphoenzyme, the conformation relaxes partially back to that of the unphosphorylated state Ca_2E1. ADP dissociation does not trigger the transition to E2P [323] as proposed previously.

12.4.2. Phosphoenzyme phosphate group

In another study, one of the ATPase phosphoenzyme intermediates (E2P) has been investigated with the aim to understand its high hydrolysis rate. The experiment has observed an oxygen isotope exchange at the phosphate group that is catalysed by the ATPase [419]. It provides an infrared spectrum at "atomic resolution" in a crowded spectral region [93,420] which reveals the three stretching vibrations of the transiently bound phosphate group in spite of a background absorption of 50,000 protein vibrations. The spectrum is shown in Fig. 6. Bands of the terminal P – O stretching vibrations of the unlabeled phosphate group are found at 1194, 1137, and 1115 cm^{-1}.

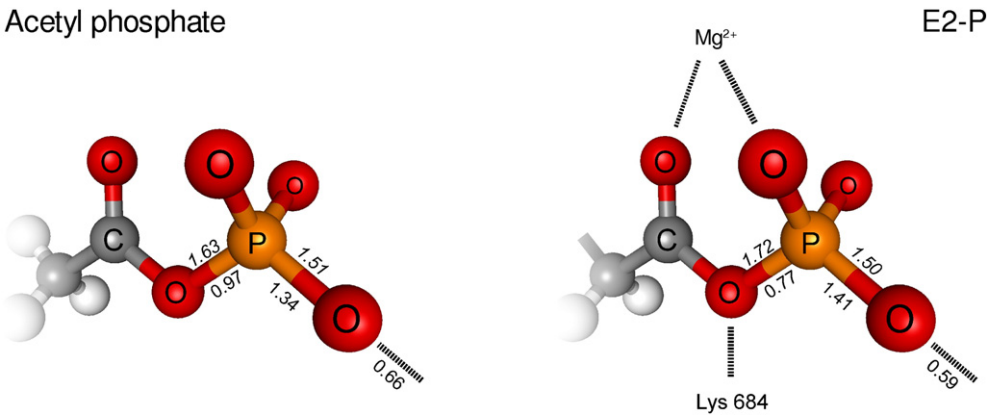

Fig. 7. Phosphate bond parameters for the model compound acetyl phosphate and E2P and a model for the phosphate group environment of E2P. Italic numbers above bonds give bond lengths in Å, normal print numbers below bonds give bond valences in vu. Reprinted from [11]. © 2006 Nova Science Publishers.

This information has been evaluated [93] using a correlation between P − O frequency and P − O bond valence [100], the bond valence model [85,421] and empirical correlations to calculate P − O bond strengths, P − O bond lengths, and finally the dissociation energy of the bridging P − O bond. Compared to the model compound acetyl phosphate, structure and charge distribution of the E2P aspartyl phosphate resemble somewhat the transition state in a dissociative phosphate transfer reaction: the aspartyl phosphate of E2P has 0.02 Å shorter terminal P − O bonds and a 0.09-Å longer bridging P − O bond which is ~20% weaker [93]. These findings are summarised in Fig. 7.

The weaker bridging P − O bond of E2-P accounts for a 10^{11}- to 10^{15}-fold hydrolysis rate enhancement implying that P − O bond destabilization facilitates phosphoenzyme hydrolysis. P − O bond destabilization is caused by a shift of non-covalent interactions from the phosphate oxygens to the aspartyl oxygens. Therefore it has been proposed [93] that the relative strength of non-covalent bonding to the phosphate and aspartyl oxygens is one of the key factors that tunes the hydrolysis rate of the ATPase phosphoenzymes and related phosphoproteins. Weaker bonding to the phosphate oxygens and stronger bonding to the aspartyl oxygens weakens the bridging P − O bond, which increases dramatically the catalytic power of the enzyme. Weakening and elongation of the bridging P − O bond is not accomplished by external mechanical forces that pull the bond apart. Instead it is an in-built response of aspartyl phosphate to a shift of interactions from phosphate to aspartyl oxygens, with only subtle changes in distances are required. This provides an elegant “handle” for the enzyme to control hydrolysis.

Acknowledgements

I am grateful for valuable discussions with Alex Perálvarey-Marín, Petra Hellwig and Peter Brzezinski.

References

[1] J.L.R. Arrondo, A. Muga, J. Castresana, F.M. Goñi, Quantitative studies of the structure of proteins in solution by Fourier-transform infrared-spectroscopy, Prog. Biophys. Mol. Biol. 59 (1993) 23–56.
[2] F. Siebert, Infrared spectroscopy applied to biochemical and biological problems, Methods Enzymol. 246 (1995) 501–526.
[3] M. Jackson, H.H. Mantsch, The use and misuse of FTIR spectroscopy in the determination of protein structure, Crit. Rev. Biochem. Mol. Biol. 30 (1995) 95–120.
[4] E. Goormaghtigh, V. Cabiaux, J.-M. Ruysschaert, Determination of soluble and membrane protein structure by Fourier transform infrared spectroscopy. I. Assignments and model compounds, Subcell, Biochemistry 23 (1994) 329–362.
[5] E. Goormaghtigh, V. Cabiaux, J.-M. Ruysschaert, Determination of soluble and membrane protein structure by Fourier transform infrared spectroscopy. II. Experimental aspects, side chain structure, and H/D exchange, Subcell. Biochem. 23 (1994) 363–403.
[6] E. Goormaghtigh, V. Cabiaux, J.-M. Ruysschaert, Determination of soluble and membrane protein structure by Fourier transform infrared spectroscopy. III. Secondary structures, Subcell. Biochem. 23 (1994) 405–450.
[7] J.L.R. Arrondo, F.M. Goñi, Structure and dynamics of membrane proteins as studied by infrared spectroscopy, Prog. Biophys. Mol. Biol. 72 (1999) 367–405.
[8] P.I. Haris, D. Chapman, Does Fourier-transform infrared spectroscopy provide useful information on protein structures? TIBS 17 (1992) 328–333.
[9] P.I. Haris, D. Chapman, Analysis of polypeptide and protein structures using Fourier transform infrared spectroscopy, in: C. Jones, B. Mulloy, A.H. Thomas (Eds.), Microscopy, Optical Spectroscopy, and Macroscopic Techniques ed., Vol. 22, Methods in Molecular Biology, Humana Press Inc, Totowa, NJ, 1994, pp. 183–202.
[10] H. Fabian, W. Mäntele, Infrared spectroscopy of proteins, in: J.M. Chalmers, P.R. Griffiths (Eds.), Handbook of Vibrational Spectroscopy, John Wiley & Sons, Chichester, 2002, pp. 3399–3426.
[11] A. Barth, IR spectroscopy, in: V.N. Uversky, E.A. Permyakov (Eds.), Protein Structures: Methods in Protein Structure and Stability Analysis, Nova Science Publishers, 2006.
[12] W. Mäntele, Infrared vibrational spectroscopy of reaction centers, in: E. Blankenship, M.T. Madigan, C.E. Bauer (Eds.), Anoxygenic Photosynthetic Bacteria, Kluwer Academic Publishers, Dordrecht, 1995, pp. 627–647.
[13] J. Breton, Fourier transform infrared spectroscopy of primary electron donors in type I photosynthetic reaction centers, Biochim. Biophys. Acta 1507 (2001) 180–193.
[14] K. Gerwert, Molecular reaction mechanisms of proteins monitored by time-resolved FTIR-spectroscopy, Biol. Chem. 380 (1999) 931–935.
[15] J. Heberle, Time-resolved ATR/FT-IR spectroscopy of membrane proteins, Recent Res. Dev. Appl. Spectrosc. 2 (1999) 147–159.
[16] A. Maeda, Application of FTIR spectroscopy to the structural study on the function of bacteriorhodopsin, Israel J. Chem. 35 (1995) 387–400.
[17] K.J. Rothschild, FTIR difference spectroscopy of bacteriorhodopsin: toward a molecular model, J. Bioenerg. Biomembr. 24 (1992) 147–167.
[18] C. Jung, Insight into protein structure and protein–ligand recognition by Fourier transform infrared spectroscopy, J. Mol. Recognit. 13 (2000) 325–351.
[19] V. Jayaraman, IR spectroscopy with caged compounds: Selected applications, in: M. Goelder, R.S. Givens (Eds.), Dynamic Studies in Biology: Phototriggers, Photoswitches and Caged Biomolecules, Wiley-VCH, Weinheim, 2005.
[20] W. Mäntele, Infrared and Fourier-transform infrared spectroscopy, in: J. Amesz, A.J. Hoff (Eds.), Biophysical Techniques in Photosynthesis, Kluwer Academic Publishers, Dordrecht, 1996, pp. 137–160.
[21] W. Mäntele, Infrared vibrational spectroscopy of the photosynthetic reaction center, in: J. Deisenhofer, J.R. Norris (Eds.), The Photosynthetic Reaction Center, Vol. 2, Academic Press, San Diego, 1993, pp. 239–283.
[22] E. Nabedryk, Light-induced Fourier transform infrared difference spectroscopy of the primary electron donor in photosynthetic reaction centers, in: H.H. Mantsch, D. Chapman (Eds.), Infrared Spectroscopy of Biomolecules, Wiley-Liss, New York, 1996, pp. 39–82.
[23] K. Gerwert, Molecular reaction mechanisms of proteins as monitored by time-resolved FTIR spectroscopy, Curr. Opin. Struct. Biol. 3 (1993) 769–773.
[24] R. Vogel, F. Siebert, Vibrational spectroscopy as a tool for probing protein function, Curr. Opin. Chem. Biol. 4 (2000) 518–523.
[25] S. Kim, B.A. Barry, Reaction-induced FT-IR spectroscopic studies of biological energy conversion in oxygenic photosynthesis and transport, J. Phys. Chem. 105 (2001) 4072–4083.
[26] K. Fahmy, Application of ATR-FTIR spectroscopy for studies of biomolecular interactions, Recent Res. Dev. Chem. 2 (2001) 1–17.
[27] C.W. Wharton, Infrared spectroscopy of enzyme reaction intermediates, Nat. Prod. Rep. 17 (2000) 447–453.
[28] W. Mäntele, Reaction-induced infrared difference spectroscopy for the study of protein function and reaction mechanisms, TIBS 18 (1993) 197–202.
[29] A. Barth, C. Zscherp, What vibrations tell us about proteins, Quart. Rev. Biophys. 35 (2002) 369–430.
[30] C. Zscherp, A. Barth, Reaction-induced infrared difference spectroscopy of the study of protein reaction mechanisms, Biochemistry 40 (2001) 1875–1883.

[31] A. Barth, C. Zscherp, Substrate binding and enzyme function investigated by infrared spectroscopy, FEBS Lett. 477 (2000) 151–156.
[32] R.B. Gennis, Some recent contributions of FTIR difference spectroscopy to the study of cytochrome oxidase, FEBS Lett. 555 (2003) 2–7.
[33] T. Noguchi, Light-induced FTIR difference spectroscopy as a powerful tool toward understanding the molecular mechanism of photosynthetic oxygen evolution, Photosynth. Res. 91 (2007) 59–69.
[34] J. Heberle, Proton transfer reactions across bacteriorhodopsin and along the membrane, Biochim. Biophys. Acta 1458 (2000) 135–147.
[35] A.K. Dioumaev, Infrared methods for monitoring the protonation state of carboxylic amino acids in the photocycle of bacteriorhodopsin, Biochemistry (Moscow) 66 (2001) 1269–1276.
[36] E. Kauffmann, N.C. Darnton, R.H. Austin, C. Batt, K. Gerwert, Lifetimes of intermediates in the ß-sheet to α-helix transitions of ß-lactoglobulin by using a diffusional IR mixer, Proc. Natl. Acad. Sci. U. S. A. 98 (2001) 6646–6649.
[37] H. Fabian, H.H. Mantsch, C.P. Schultz, Two-dimensional IR correlation spectroscopy: Sequential events in the unfolding process of the lambda Cro-V55C repressor protein, Proc. Natl. Acad. Sci. U. S. A. 96 (1999) 13153–13158.
[38] D. Reinstädler, H. Fabian, D. Naumann, New structural insights into the refolding of ribonuclease T1 as seen by time-resolved Fourier-transform infrared spectroscopy, Proteins 34 (1999) 303–316.
[39] S. Williams, T.P. Causgrove, R. Gilmanshin, K.S. Fang, R.H. Callender, W.H. Woodruff, R.B. Dyer, Fast events in protein folding: helix melting and formation in a small peptide, Biochemistry 335 (1996) 691–697.
[40] R. Gilmanshin, S. Williams, R.H. Callender, W.H. Woodruff, R.B. Dyer, Fast events in protein folding: relaxation dynamics and structure of the I form of apomyoglobin, Biochemistry 36 (1997) 15006–15012.
[41] C.P. Schultz, Illuminating folding intermediates, Nat. Struct. Biol. 7 (2000) 7–10.
[42] A. Troullier, D. Reinstädler, Y. Dupont, D. Naumann, V. Forge, Transient non-native secondary structures during the refolding of α-lactalbumin detected by infrared spectroscopy, Nat. Struct. Biol. 7 (2000) 78–86.
[43] R.B. Dyer, F. Gai, W.H. Woodruff, R. Gilmanshin, R.H. Callender, Infrared studies of fast events in protein folding, Acc. Chem. Res. 31 (1998) 709–716.
[44] A.P. Ramajo, S.A. Petty, A. Starzyk, S.M. Decatur, M. Volk, The α-helix folds more rapidly at the C-terminus than at the N-terminus, J. Am. Chem. Soc. 127 (2005) 13784–13785.
[45] D. Naumann, FT-infrared and FT-Raman spectroscopy in biomedical research, in: H.U. Gremlich, B. Yan (Eds.), Infrared and Raman Spectroscopy of Biological Materials, Marcel Dekker Inc., New York, 2001, pp. 323–377.
[46] M. Diem, M. Romeo, S. Boydston-White, M. Miljkovic, C. Matthaus, A decade of vibrational micro-spectroscopy of human cells and tissue (1994–2004), Analyst 129 (2004) 880–885.
[47] R. Salzer, G. Steiner, H.H. Mantsch, J. Mansfield, E.N. Lewis, Infrared and Raman imaging of biological and biomimetic samples, Fresenius J. Anal. Chem. 366 (2000) 712–726.
[48] M. Jackson, M.G. Sowa, H.H. Mantsch, Infrared spectroscopy: a new frontier in medicine, Biophys. Chem. 68 (1997) 109–125.
[49] S.-Y. Lin, M.-J. Li, W.-T. Cheng, FT-IR and Raman vibrational microspectroscopies used for spectral biodiagnosis of human tissues, Spectroscopy 21 (2007) 1–30.
[50] K.C. Schultz, L. Supekova, Y. Ryu, J. Xie, R. Perera, P.G. Schultz, A genetically encoded infrared probe, J. Am. Chem. Soc. 128 (2006) 13984–13985.
[51] I. Mills, T. Cvitas, K. Homann, N. Kallay, K. Kuchitsu, Quantities, Units and Symbols in Physical Chemistry, Blackwell Scientific Publications, Oxford, 1988.
[52] A.A. Lamola, M.S. Wrighton, Recommended standards for reporting photochemical data, Pure Appl. Chem. 56 (1984) 939–944.
[53] H. Deng, R. Callender, Raman spectroscopic studies of the structures, energetics, and bond distortions of substrates bound to enzymes, Methods Enzymol. 308 (1999) 176–201.
[54] R. Callender, H. Deng, Nonresonance Raman difference spectroscopy: a general probe of protein structure, ligand binding, enzymatic catalysis, and the structures of other biomacromolecules, Annu. Rev. Biophys. Biomol. Struct. 23 (1994) 215–245.
[55] P.R. Carey, Raman spectroscopy in enzymology: the first 25 years, J. Raman Spectrosc. 29 (1998) 7–14.
[56] P.R. Carey, Raman spectroscopy, the sleeping giant in structural biology, awakes, J. Biol. Chem. 274 (1999) 26625–26628.
[57] T.G. Spiro, B.P. Gaber, Laser Raman scattering as a probe of protein structure, Annu. Rev. Biochem. 46 (1977) 553–572.
[58] B. Robert, Resonance Raman studies in photosynthesis—Chlorophyll and carotenoid molecules, in: J. Amesz, A.J. Hoff (Eds.), Biophysical Techniques in Photosynthesis, 1996, pp. 161–176.
[59] H. Deng, R. Callender, Vibrational studies of enzymatic catalysis, in: H.U. Gremlich, B. Yan (Eds.), Infrared and Raman Spectroscopy of Biological Materials, Marcel Dekker Inc., New York, 2001, pp. 477–515.
[60] G.J. Thomas Jr., New structural insights from Raman spectroscopy of proteins and their assemblies, Biopolymers (Biospectroscopy) 67 (2002) 214–225.
[61] P.R. Carey, P.J. Tonge, Unlocking the secrets of enzyme power using Raman spectroscopy, Acc. Chem. Res. 28 (1995) 8–13.
[62] A. Barth, W. Mäntele, W. Kreutz, Ca^{2+} release from the phosphorylated and the unphosphorylated sarcoplasmic reticulum Ca^{2+} ATPase results in parallel structural changes. An infrared spectroscopic study, J. Biol. Chem. 272 (1997) 25507–25510.
[63] F. Von Germar, A. Barth, W. Mäntele, Structural changes of the sarcoplasmic reticulum Ca^{2+}-ATPase upon nucleotide binding studied by Fourier transform infrared spectroscopy, Biophys. J. 78 (2000) 1531–1540.
[64] R. Hienerwadel, A. Boussac, J. Breton, B. Diner, C. Berthomieu, Fourier transform infrared difference spectroscopy of photosystem II tyrosine D using site-directed mutagenesis and specific isotope labeling, Biochemistry 36 (1997) 14712–14723.
[65] T. Noguchi, Y. Inoue, X.-S. Tang, Structure of a histidine ligand in the photosynthetic oxygen-evolving complex as studied by light-induced Fourier transform infrared difference spectroscopy, Biochemistry 38 (1999) 10187–10195.
[66] G. Dollinger, L. Eisenstein, L. Shuo-Liang, K. Nakanishi, J. Termini, Fourier transform infrared difference spectroscopy of bacteriorhodopsin and its photoproducts regenerated with deuterated tyrosine, Biochemistry 25 (1986) 6524–6533.
[67] K.J. Rothschild, P. Roepe, P.L. Ahl, T.N. Earnest, R.A. Bogomolni, S.K. Das Gupta, C.M. Mulliken, J. Herzfeld, Evidence for a tyrosine protonation change during the primary phototransition of bacteriorhodopsin at low temperature, Proc. Natl. Acad. Sci. U. S. A. 83 (1986) 347–351.
[68] P. Roepe, P.L. Ahl, S.K. Das Gupta, J. Herzfeld, K.J. Rothschild, Tyrosine and carboxyl protonation changes in the bacteriorhodopsin photocycle. 1. M412 and L550 intermediates, Biochemistry 26 (1987) 6696–6707.
[69] A. Barth, W. Mäntele, ATP-induced phosphorylation of the sarcoplasmic reticulum Ca^{2+} ATPase: Molecular interpretation of infrared difference spectra, Biophys. J. 75 (1998) 538–544.
[70] A. Barth, Phosphoenzyme conversion of the sarcoplasmic reticulum Ca^{2+}-ATPase. Molecular interpretation of infrared difference spectra, J. Biol. Chem. 274 (1999) 22170–22175.
[71] A. Barth, W. Mäntele, W. Kreutz, Infrared spectroscopic signals arising from ligand binding and conformational changes in the catalytic cycle of sarcoplasmic reticulum Ca^{2+}-ATPase, Biochim. Biophys. Acta 1057 (1991) 115–123.
[72] D. Thoenges, A. Barth, Direct measurement of enzyme activity with infrared spectroscopy, J. Biomol. Screen. 7 (2002) 353–357.
[73] C. Raimbault, E. Clottes, C. Leydier, C. Vial, R. Buchet, ADP-binding and ATP-binding sites in native and proteinase-K-digested creatine kinase, probed by reaction-induced difference infrared spectroscopy, Eur. J. Biochem. 247 (1997) 1197–1208.
[74] K. Karmali, A. Karmali, A. Teixeira, M.J.M. Curto, Assay for glucose oxidase from *Aspergillus niger* and *Penicillium amagasakiense* by Fourier transform infrared spectroscopy, Anal. Biochem. 333 (2004) 320–327.

[75] R. Schindler, B. Lendl, FTIR spectroscopy as detection principle in aqueous flow analysis, Anal. Commun. 36 (1999) 123–126.
[76] R. Pacheco, M.L.M. Serralheiro, A. Karmali, P.I. Haris, Measuring enzymatic activity of a recombinant amidase using Fourier transform infrared spectroscopy, Anal. Biochem. 322 (2003) 208–214.
[77] J. Fisher, J.G. Belasco, S. Khosla, J.R. Knowles, ß-Lactamase proceeds via an acyl-enzyme intermediate. Interaction of the *Escherichia coli* RTEM enzyme with cefoxitin, Biochemistry 19 (1980) 2895–2901.
[78] A.J. White, K. Drabble, S. Ward, C.W. Wharton, Analysis and elimination of protein perturbation in infrared difference spectra of acyl-chymotrypsin ester carbonyl groups by using ^{13}C isotopic substitution, Biochem. J. 287 (1992) 317–323.
[79] N.B. Colthup, L.H. Daly, S.E. Wiberley, Introduction to Infrared and Raman Spectroscopy, 2nd ed.Academic Press, New York, 1975.
[80] W.G. Mäntele, A.M. Wollenweber, E. Nabedryk, J. Breton, Infrared spectroelectrochemistry of bacteriochlorophylls and bacteriopheophytins: Implications for the binding of the pigments in the reaction center from photosynthetic bacteria, Proc. Natl. Acad. Sci. U. S. A. 85 (1988) 8468–8472.
[81] M. Bauscher, E. Nabedryk, K. Bagley, J. Breton, W. Mäntele, Investigation of models for photosynthetic electron acceptors. Infrared spectroelectrochemistry of ubiquinone and its anions, FEBS Lett. 261 (1990) 191–195.
[82] E. Nabedryk, M. Leonhard, W. Mäntele, J. Breton, Fourier transform infrared difference spectroscopy shows no evidence for an enolization of chlorophyll *a* upon cation formation either in vitro or during P700 photooxidation, Biochemistry 29 (1990) 3242–3247.
[83] M. Bauscher, W. Mäntele, Electrochemical and infrared-spectroscopic characterization of redox reactions of *p*-quinones, J. Phys. Chem. 96 (1992) 11101–11108.
[84] M.A. Palafox, Empirical correlations in vibrational spectroscopy, Trends Appl. Spectrosc. 2 (1998) 37–57.
[85] I.D. Brown, The Chemical Bond in Inorganic Chemistry. The Bond Valence Model, Oxford University Press, Oxford, 2002.
[86] R. Allmann, Beziehungen zwischen Bindungslängen und Bindungsstärken in Oxidstrukturen, Monatshefte für Chemie 106 (1975) 779–793.
[87] P.J. Tonge, P.R. Carey, Length of the acyl carbonyl bond in acyl-serine proteases correlates with reactivity, Biochemistry 29 (1990) 10723–10727.
[88] A.J. White, C.W. Wharton, Hydrogen-bonding in enzyme catalysis. Fourier-transform infrared detection of ground-state electronic strain in acyl-chymotrypsins and analysis of the kinetic consequences, Biochem. J. 270 (1990) 627–637.
[89] H. Deng, J. Wang, R.H. Callender, J.C. Grammer, R.G. Yount, Raman difference spectroscopic studies of the myosin S1·MgADP·vanadate complex, Biochemistry 37 (1998) 10972–10979.
[90] J.H. Wang, D.G. Xiao, H. Deng, M.R. Webb, R. Callender, Raman difference studies of GDP and GTP binding to c-Harvey ras, Biochemistry 37 (1998) 11106–11116.
[91] H. Cheng, S. Sukal, H. Deng, T.S. Leyh, R. Callender, Vibrational structure of GDP and GTP bound to RAS: an isotope-edited FTIR study, Biochemistry 40 (2001) 4035–4043.
[92] M. Klähn, J. Schlitter, K. Gerwert, Theoretical IR spectroscopy based on QM/MM calculations provides changes in charge distribution, bond lengths, and bond angles of the GTP ligand induced by the Ras-protein, Biophys. J. 88 (2005) 3829–3844.
[93] A. Barth, N. Bezlyepkina, P−O bond destabilization accelerates phosphoenzyme hydrolysis of sarcoplasmic reticulum Ca^{2+}-ATPase, J. Biol. Chem. 279 (2004) 51888–51896.
[94] J. Andersson, A. Barth, FTIR studies on the bond properties of the aspartyl phosphate moiety of the Ca^{2+}-ATPase, Biopolymers 82 (2006) 353–357.
[95] G.B. Deacon, R.J. Phillips, Relationships between the carbon-oxygen stretching frequencies of carboxylate complexes and the type of carboxylate coordination, Coord. Chem. Rev. 33 (1980) 227–250.
[96] J.E. Tackett, FT-IR characterisation of metal acetates in aqueous solution, Appl. Spectrosc. 43 (1989) 483–489.
[97] M. Nara, H. Torii, M. Tasumi, Correlation between the vibrational frequencies of the carboxylate group and the types of its coordination to a metal ion: an ab initio molecular orbital study, J. Phys. Chem. 100 (1996) 19812–19817.
[98] M. Mizuguchi, M. Nara, K. Kawano, K. Nitta, FT-IR study of the calcium-binding to bovine α-lactalbumin. Relationships between the type of coordination and characteristics of the bands due to the Asp carboxylate groups in the calcium binding site, FEBS Lett. 417 (1997) 153–156.
[99] M. Nara, M. Tasumi, M. Tanokura, T. Hiraoki, M. Yazawa, A. Tsutsumi, Infrared studies of interaction between metal ions and Ca^{2+} binding proteins. Marker bands for identifying the types of coordination of the side-chain carboxylate groups to metal ions in pike parvalbumin (pI=4.10), FEBS Lett. 349 (1994) 84–88.
[100] H. Deng, J. Wang, R. Callender, W.J. Ray, Relationship between bond stretching frequencies and internal bonding for [$^{16}O_4$]- and [$^{18}O_4$] phosphates in aqueous solution, J. Phys. Chem., B 102 (1998) 3617–3623.
[101] G. Maes, T. Zeegers-Huyskens, Matrix isolation infrared spectra of the complexes between methylacetate and water or hydrochloric acid, J. Mol. Struct. 100 (1983) 305–315.
[102] G. Maes, A. Smolders, P. Vandevyvere, L. Vanderheyden, T. Zeegers-Huyskens, Matrix-isolation IR studies on the basic interaction sites in esters and thiolesters towards proton donors, J. Mol. Struct. 173 (1988) 349–356.
[103] A.K. Dioumaev, M.S. Braiman, Modeling vibrational spectra of amino acid side chains in proteins: The carbonyl stretch frequency of buried carboxylic residues, J. Am. Chem. Soc. 117 (1995) 10572–10574.
[104] E.B. Brown, W.L. Peticolas, Conformational geometry and vibrational frequencies of nucleic acid chains, Biopolymers 14 (1975) 1259–1271.
[105] J.L.R. Arrondo, F.M. Goñi, J.M. Macarulla, Infrared spectroscopy of phosphatidylcholines in aqueous suspension. A study of the phosphate group vibrations, Biochim. Biophys. Acta 794 (1984) 165–168.
[106] W. Pohle, M. Bohl, H. Böhlig, Interpretation of the influence of hydrogen bonding on the stretching vibrations of the PO_2^- moiety, J. Mol. Struct. 242 (1990) 333–342.
[107] L. George, K. Sankaran, K.S. Viswanathan, C.K. Mathews, Matrix-isolation infrared spectroscopy of hydrogen-bonded complexes of triethyl phosphate with H_2O, D_2O, and methanol, Appl. Spectrosc. 48 (1994) 801–807.
[108] R.M. Badger, S.H. Bauer, Spectroscopic studies of the hydrogen bond. II. The shift of the O−H vibrational frequency in the formation of the hydrogen bond, J. Chem. Phys. 5 (1937) 839–851.
[109] M.D. Joesten, L.J. Schaad, Hydrogen Bonding, Marcel Dekker Inc, New York, 1974.
[110] P.J. Tonge, R. Fausto, P.R. Carey, FTIR studies of hydrogen bonding between α,ß-unsaturated esters and alcohols, J. Mol. Struct. 379 (1996) 135–142.
[111] M.T. Zanni, M.C. Asplund, R.M. Hochstrasser, Two-dimensional heterodyned and stimulated infrared photon echoes of *N*-methylacetamide-D, J. Chem. Phys. 114 (2001) 4579–4590.
[112] S. Hahn, S. Ham, M. Cho, Simulation studies of amide I IR absorption and two-dimensional IR spectra of ß hairpins in liquid water, J. Phys. Chem. 109 (2005) 11789–11801.
[113] TlC. Jansen, J. Knoester, A transferable electrostatic map for solvation effects on amide I vibrations and its application to linear and two-dimensional spectroscopy, J. Chem. Phys. 124 (2006) 044502.
[114] V. Cepus, A.J. Scheidig, R.S. Goody, K. Gerwert, Time-resolved FTIR studies of the GTPase reaction of H-*ras* p21 reveal a key role for the ß-phosphate, Biochemistry 37 (1998) 10263–10271.
[115] P. Hellwig, T. Mogi, F.L. Tomson, R.B. Gennis, J. Iwata, H. Miyoshi, W. Mäntele, Vibrational modes of ubiquinone in cytochrome bo_3 from *Escherichia coli* identified by Fourier transform infrared difference spectroscopy and specific ^{13}C labeling, Biochemistry 38 (1999) 14683–14689.
[116] M. Iwaki, N.P.J. Cotton, P.G. Quirk, P.R. Rich, J.B. Jackson, Molecular recognition between protein and nicotinamide dinucleotide in intact, proton-translocating transhydrogenase studied by ATR-FTIR spectroscopy, J. Am. Chem. Soc. 128 (2006) 2621–2629.

[117] P. Hinsmann, M. Haberkorn, J. Frank, P. Svasek, M. Harasek, B. Lendl, Time-resolved FT-IR spectroscopy of chemical reactions in solution by fast diffusion-based mixing in a micromachined flow cell, Appl. Spectrosc. 55 (2001) 241–251.
[118] A.J. White, K. Drabble, C.W. Wharton, A stopped-flow apparatus for infrared spectroscopy of aqueous solutions, Biochem. J. 306 (1995) 843–849.
[119] R. Masuch, D.A. Moss, Stopped flow system for FTIR difference spectroscopy of biological macromolecules, in: J. Greve, G.J. Puppels, C. Otto (Eds.), Spectroscopy of Biological Molecules: New Directions, Kluwer Academic Publishers, Dordrecht, 1999, pp. 689–690.
[120] S.Y. Venyaminov, F.G. Prendergast, Water (H_2O and D_2O) molar absorptivity in the 1000–4000 cm^{-1} range and quantitative infrared spectroscopy of aqueous solutions, Anal. Biochem. 248 (1997) 234–245.
[121] K.A. Oberg, A.L. Fink, A new attenuated total reflectance Fourier transform infrared spectroscopy method for the study of proteins in solution, Anal. Biochem. 256 (1998) 92–106.
[122] P. Rigler, W.P. Ulrich, R. Hovius, E. Ilegems, H. Pick, H. Vogel, Downscaling Fourier transform infrared spectroscopy to the micrometer and nanogram scale: secondary structure of serotonin and acetylcholine receptors, Biochemistry 42 (2003) 14017–14022.
[123] K. Ataka, J. Heberle, Biochemical applications of surface-enhanced infrared absorption spectroscopy, Anal. Bioanal. Chem. 388 (2007) 47–54.
[124] U.P. Fringeli, In situ infrared attenuated total reflection membrane spectroscopy, in: F.M.J. Mirabella (Ed.), Internal Reflection Spectroscopy, Marcel Dekker, Inc., New York, 1992, pp. 255–324.
[125] E. Goormaghtigh, V. Raussens, J.-M. Ruysschaert, Attenuated total reflection infrared spectroscopy of proteins and lipids in biological membranes, Biochim. Biophys. Acta 1422 (1999) 105–185.
[126] L.K. Tamm, S.A. Tatulian, Infrared spectroscopy of proteins and peptides in lipid bilayers, Quart. Rev. Biophys. 30 (1997) 365–429.
[127] P. Rigler, W.P. Ulrich, P. Hoffmann, M. Mayer, H. Vogel, Reversible immobilization of peptides: Surface modification and in situ detection by attenuated total reflection FTIR Spectroscopy, ChemPhysChem 4 (2003) 268–275.
[128] P. Rigler, W.P. Ulrich, H. Vogel, Controlled immobilization of membrane proteins to surfaces for Fourier transform infrared investigations, Langmuir 20 (2004) 7901–7903.
[129] K. Fahmy, Binding of transducin and transducin-derived peptides to rhodopsin studied by attenuated total reflection-Fourier transform infrared difference spectroscopy, Biophys. J. 75 (1998) 1306–1318.
[130] E. Agic, O. Klein, W. Mäntele, Binding and interaction of effector molecules to proteins studied with an attenuated total reflection infrared (ATR-IR) microdialysis cell, in: B. Szalontai, Z. Kóta (Eds.), Book of Abstracts: 10th European Conference on the Spectroscopy of Biological Molecules, JATE Press, Szeged, 2003, p. 93.
[131] S. Gourion-Arsiquaud, S. Chevance, P. Bouyer, L. Garnier, J.-L. Montillet, A. Bondon, C. Berthomieu, Identification of a Cd^{2+}- and Zn^{2+}-binding site in cytochrome *c* using FTIR coupled to an ATR microdialysis setup and NMR spectroscopy, Biochemistry 44 (2005) 8652–8663.
[132] M. Krasteva, S. Kumar, A. Barth, A dialysis accessory for attenuated total reflection infrared spectroscopy, Spectroscopy 20 (2006) 89–94.
[133] F. Siebert, Equipment: slow and fast infrared kinetic studies, in: H.H. Mantsch, D. Chapman (Eds.), Infrared Spectroscopy of Biomolecules, Wiley-Liss. Inc, New York, 1996, pp. 83–106.
[134] B.R. Cowen, R.M. Hochstrasser, Ultrafast infrared spectroscopy of biomolecules, in: H.H. Mantsch, D. Chapman (Eds.), Infrared Spectroscopy of Biomolecules, Wiley-Liss. Inc., New York, 1996, pp. 107–129.
[135] R.M. Slayton, P.A. Anfinrud, Time-resolved mid-infrared spectroscopy: methods and biological applications, Curr. Opin. Struct. Biol. 7 (1997) 717–721.
[136] M. Tasumi, Present status of time-resolved vibrational spectroscopy, J. Mol. Struct. 292 (1993) 289–293.
[137] H. Georg, K. Hauser, C. Rödig, O. Weidlich, F. Siebert, Time-resolved infrared spectroscopy of biomolecules, NATO ASI Ser., Ser. E: Appl. Sci. 342 (1997) 243–261.
[138] H. Frei, Nanosecond step-scan FT-infrared absorption spectroscopy in photochemistry and catalysis, AIP Conf. Proc. 430 (1998) 28–39.
[139] E. Hirota, K. Kawaguchi, High resolution infrared studies of molecular dynamics, Annu. Rev. Phys. Chem. 36 (1985) 53–76.
[140] M.W. George, M. Poliakoff, J.J. Turner, Nanosecond time-resolved infrared spectroscopy: a comparative view of spectrometers and their applications in organometallic chemistry, Analyst 119 (1994) 551–560.
[141] K. McFarlane, B. Lee, J. Bridgewater, P.C. Ford, Time resolved infrared spectroscopy as a technique to study reactive organometallic intermediates, J. Organomet. Chem. 554 (1998) 49–61.
[142] J.P. Toscano, Structure and reactivity of organic intermediates as revealed by time-resolved infrared spectroscopy, Adv. Photochem. 26 (2001) 41–91.
[143] M.T. Zanni, R.M. Hochstrasser, Two-dimensional infrared spectroscopy: a promising new method for the time resolution of structures, Curr. Opin. Struct. Biol. 11 (2001) 516–522.
[144] W. Uhmann, A. Becker, C. Taran, F. Siebert, Time-resolved FT-IR absorption spectroscopy using a step-scan interferometer, Appl. Spectrosc. 45 (1991) 390–397.
[145] R. Rammelsberg, S. Boulas, H. Chorongiewski, K. Gerwert, Set-up for time-resolved step-scan FTIR spectroscopy of noncyclic reactions, Vibr. Spectrosc. 19 (1999) 143–149.
[146] Q. Cheng, M.G. Steinmetz, V. Jayaraman, Photolysis of γ-(α-carboxy-2-nitrobenzyl)-L-glutamic acid investigated in the microsecond time scale by time-resolved FTIR, J. Am. Chem. Soc. 124 (2002) 7676–7677.
[147] R.B. Dyer, Ó. Einarsdóttir, P.M. Killough, J.J. López-Garriga, W.H. Woodruff, Transient binding of photodissociated CO to Cu_B^+ of eukaryotic cytochrome oxidase at ambient temperature. Direct evidence from time-resolved infrared spectroscopy, J. Am. Chem. Soc. 111 (1989) 7657–7659.
[148] W. Mäntele, R. Hienerwadel, F. Lenz, W.J. Riedel, R. Grisar, M. Tacke, Application of tunable infrared diode lasers for the study of biochemical reactions: time-resolved vibrational spectroscopy of intermediates in the primary processes of photosynthesis, Spectrosc. Int. 2 (1990) 29–35.
[149] T. Yuzawa, C. Kato, M.W. George, H. Hamaguchi, Nanosecond time-resolved infrared spectroscopy with a dispersive scanning spectrometer, Appl. Spectrosc. 48 (1994) 684–690.
[150] A. Barth, The infrared absorption of amino acid side chains, Prog. Biophys. Mol. Biol. 74 (2000) 141–173.
[151] S. Krimm, J. Bandekar, Vibrational spectroscopy and conformation of peptides, polypeptides, and proteins, Adv. Prot. Chem. 38 (1986) 181–367.
[152] K. Rahmelow, W. Hübner, T. Ackermann, Infrared absorbances of protein side chains, Anal. Biochem. 257 (1998) 1–11.
[153] W. Wright, J.M. Vanderkooi, Use of IR absorption of the carboxyl group of amino acids and their metabolites to determine pKs, to study proteins, and to monitor enzymatic activity, Biospectroscopy 3 (1997) 457–467.
[154] S.Y. Venyaminov, N.N. Kalnin, Quantitative IR spectrophotometry of peptide compounds in water (H_2O) solutions. I. Spectral parameters of amino acid residue absorption bands, Biopolymers 30 (1990) 1243–1257.
[155] Y.N. Chirgadze, O.V. Fedorov, N.P. Trushina, Estimation of amino acid residue side chain absorption in the infrared spectra of protein solutions in heavy water, Biopolymers 14 (1975) 679–694.
[156] M. Wolpert, P. Hellwig, Infrared spectra and molecular absorption coefficients of the 20 alpha amino acids in aqueous solutions in the spectral range from 1800 to 500 cm^{-1}, Spectrochim. Acta, A Mol. Spectrosc. 64 (2006) 987–1001.
[157] R.C. Lord, N.-T. Yu, Laser-excited Raman spectroscopy of biomolecules. II Native ribonuclease and α-chymotrypsin, J. Mol. Biol. 51 (1970) 203–213.
[158] R.C. Lord, N.-T. Yu, Laser-excited Raman spectroscopy of biomolecules. I. Native lysozyme and its constituent amino acids, J. Mol. Biol. 50 (1970) 509–524.
[159] R.P. Rava, T.G. Spiro, Resonance enhancement in the ultraviolet Raman spectra of aromatic amino acids, J. Phys. Chem. 89 (1985) 1856–1861.
[160] S.A. Asher, M. Ludwig, C.R. Johnson, UV resonance Raman excitation profiles of the aromatic amino acids, J. Am. Chem. Soc. 108 (1986) 3186–3197.

[161] S.A. Overman, G.J. Thomas, Raman markers of nonaromatic side chains in an α-helix assembly: Ala, Asp, Glu, Gly, Ile, Leu, Lys, Ser, and Val residues of phage *fd* subunits, Biochemistry 38 (1999) 4018–4027.
[162] P. Lagant, G. Vergoten, W.L. Peticolas, On the use of ultraviolet resonance Raman intensities to elaborate molecular force fields: application to nucleic acid bases and aromatic amino acid residues models, Biospectroscopy 4 (1998) 379–393.
[163] C. Zscherp, R. Schlesinger, J. Tittor, D. Oesterhelt, J. Heberle, In situ determination of transient pK_a changes of internal amino acids of bacteriorhodopsin by using time-resolved attenuated total reflection Fourier-transform infrared spectroscopy, Proc. Natl. Acad. Sci. U. S. A. 96 (1999) 5498–5503.
[164] Y. Wang, K. Murayama, Y. Myojo, R. Tsenkova, N. Hayashi, Y. Ozaki, Two-dimensional Fourier transform near-infrared spectroscopy study of heat denaturation of ovalbumin in aqueous solutions, J. Phys. Chem., B 102 (1998) 6655–6662.
[165] K.A. Oberg, J.M. Ruysschaert, E. Goormaghtigh, The optimization of protein secondary structure determination with infrared and circular dichroism spectra, Eur. J. Biochem. 271 (2004) 2937–2948.
[166] M.X. Xie, Y. Liu, Studies on amide III infrared bands for the secondary structure determination of proteins, Chem. J. Chin. Univ.—Chinese 24 (2003) 226–231.
[167] F.N. Fu, D.B. Deoliveira, W.R. Trumble, H.K. Sarkar, B.R. Singh, Secondary structure estimation of proteins using the amide-III region of Fourier-transform infrared-spectroscopy—Application to analyze calcium binding-induced structural-changes in calsequestrin, Appl. Spectrosc. 48 (1994) 1432–1441.
[168] S. Cai, B.R. Singh, Identification of ß-turn and random coil amide III infrared bands for secondary structure estimation of proteins, Biophys. Chem. 80 (1999) 7–20.
[169] S. Cai, B.R. Singh, A distinct utility of the amide III infrared band for secondary structure estimation of aqueous protein solutions using partial least squares methods, Biochemistry 43 (2004) 2541–2549.
[170] Y. Abe, S. Krimm, Normal vibrations of crystalline polyglycine I, Biopolymers 11 (1972) 1817–1839.
[171] H. Torii, T. Tatsumi, M. Tasumi, Effects of hydration on the structure, vibrational wavenumbers, vibrational force field and resonance Raman intensities of *N*-methylacetamide, J. Raman Spectrosc. 29 (1998) 537–546.
[172] M. Jackson, H.H. Mantsch, Protein secondary structure from FT-IR spectroscopy: correlation with dihedral angles from three-dimensional Ramachandran plots, Can. J. Chem. 69 (1991) 1639–1642.
[173] S. Krimm, Y. Abe, Intermolecular interaction effects in the amide I vibrations of ß polypeptides, Proc. Natl. Acad. Sci. U. S. A. 69 (1972) 2788–2792.
[174] N.A. Nevskaya, Y.N. Chirgadze, Infrared spectra and resonance interactions of amide-I and II vibrations of α-helix, Biopolymers 15 (1976) 637–648.
[175] Y.N. Chirgadze, N.A. Nevskaya, Infrared spectra and resonance interaction of amide-I vibration of the parallel-chain pleated sheet, Biopolymers 15 (1976) 627–636.
[176] Y.N. Chirgadze, N.A. Nevskaya, Infrared spectra and resonance interaction of amide-I vibration of the antiparallel-chain pleated sheet, Biopolymers 15 (1976) 607–625.
[177] R. Schweitzer-Stenner, Advances in vibrational spectroscopy as a sensitive probe of peptide and protein structure. A critical review, Vibr. Spectrosc. 42 (2006) 98–117.
[178] P. Hamm, M. Lim, R.M. Hochstrasser, Structure of the amide I band of peptides measured by femtosecond nonlinear-infrared spectroscopy, J. Phys. Chem., B 102 (1998) 6123–6138.
[179] Y.N. Chirgadze, B.V. Shestopalov, S.Y. Venyaminov, Intensities and other spectral parameters of infrared amide bands of polypeptides in the ß- and random forms, Biopolymers 12 (1973) 1337–1351.
[180] S.Y. Venyaminov, N.N. Kalnin, Quantitative IR spectroscopy of peptide compounds in water (H_2O) solutions. II Amide absorption bands of polypeptides and fibrous proteins in α-, ß-, and random coil conformations, Biopolymers 30 (1990) 1259–1271.
[181] S. Cha, S. Ham, M. Cho, Amide I vibrational modes in glycine dipeptide analog: ab initio calculation studies, J. Chem. Phys. 117 (2002) 740–750.
[182] J. Kubelka, J. Kim, P. Bour, T.A. Keiderling, Contribution of transition dipole coupling to amide coupling in IR spectra of peptide secondary structures, Vibr. Spectrosc. 42 (2006) 63–73.
[183] R. Huang, J. Kubelka, W. Barber-Armstrong, R.A.G.D. Silva, S.M. Decatur, T.A. Keiderling, Nature of vibrational coupling in helical peptides: an isotopic labeling study, J. Am. Chem. Soc. 126 (2004) 2346–2354.
[184] P. Hamm, M. Lim, W.F. DeGrado, R.M. Hochstrasser, The two-dimensional IR nonlinear spectroscopy of a cyclic penta-peptide in relation to its three-dimensional structure, Proc. Natl. Acad. Sci. U. S. A. 96 (1999) 2036–2041.
[185] H. Torii, M. Tasumi, Ab initio molecular orbital study of the amide I vibrational interactions between the peptide groups in di- and tripeptides and considerations on the conformation of the extended helix, J. Raman Spectrosc. 229 (1998) 81–86.
[186] J. Antony, B. Schmidt, C. Schütte, Nonadiabatic effects on peptide vibrational dynamics induced by conformational changes, J. Chem. Phys. 122 (2005) 014309.
[187] R.D. Gorbunov, G. Stock, Ab initio based building block model of amide I vibrations in peptides, Chem. Phys. Lett. 437 (2007) 272–276.
[188] J.W. Brauner, C. Dugan, R. Mendelsohn, ^{13}C isotope labeling of hydrophobic peptides. Origin of the anomalous intensity distribution in the infrared amide I spectral region of ß-sheet structures, J. Am. Chem. Soc. 122 (2000) 677–683.
[189] H. Torii, T. Tatsumi, T. Kanazawa, M. Tasumi, Effects of intermolecular hydrogen-bonding interactions on the amide I mode of *N*-methylacetamide: matrix-isolation infrared studies and ab initio molecular orbital calculations, J. Phys. Chem., B 102 (1998) 309–314.
[190] B. Mennucci, J.M. Martinez, How to model solvation of peptides? Insights from a quantum-mechanical and molecular dynamics study of *N*-methylacetamide. I. Geometries, infrared, and ultraviolet spectra in water, J. Phys. Chem. 109 (2005) 9818–9829.
[191] J. Kubelka, T.A. Keiderling, Ab initio calculation of amide carbonyl stretch vibrational frequencies in solution with modified basis sets. 1. *N*-methyl acetamide, J. Phys. Chem., A 105 (2001) 10922–10928.
[192] W.C. Reisdorf, S. Krimm, Infrared amide I′ band of the coiled coil, Biochemistry 35 (1996) 1383–1386.
[193] J.R. Parrish, E.R. Blout, The conformation of poly-L-alanine in hexafluoroisopropanol, Biopolymers 11 (1972) 1001–1020.
[194] E.S. Manas, Z. Getahun, W.W. Wright, W.F. DeGrado, J.M. Vanderkooi, Infrared spectra of amide groups in α-helical proteins: evidence for hydrogen bonding between helices and water, J. Am. Chem. Soc. 122 (2000) 9883–9890.
[195] S.T.R. Walsh, R.P. Cheng, W.W. Wright, D.O.V. Alonso, V. Daggett, J.M. Vanderkooi, W.F. DeGrado, The hydration of amides in helices; a comprehensive picture from molecular dynamics, IR, and NMR, Protein Sci. 12 (2003) 520–531.
[196] C. Jansen, A.G. Dijkstra, T.M. Watson, J.D. Hirst, J. Knoester, Modeling the amide I bands of small peptides, J. Chem. Phys. 125 (2006) 044312.
[197] S. Ham, J.-H. Kim, H. Lee, M. Cho, Correlation between electronic and molecular structure distortions and vibrational properties. II. Amide I modes of NMA–$n$$D_2O$ complexes, J. Chem. Phys. 118 (2003) 3491–3498.
[198] S. Ham, M. Cho, Amide I modes in the *N*-methylacetamide dimer and glycine dipeptide analog: diagonal force constants, J. Chem. Phys. 118 (2003) 6915–6922.
[199] P. Bour, T.A. Keiderling, Empirical modeling of the peptide amide I band IR intensity in water solution, J. Chem. Phys. 119 (2003) 11253–11262.
[200] J.R. Schmidt, S.A. Corcelli, J.L. Skinner, Ultrafast vibrational spectroscopy of water and aqueous *N*-methylacetamide: comparison of different electronic structure/molecular dynamics approaches, J. Chem. Phys. 121 (2004) 8887–8896.
[201] T. Hayashi, W. Zhuang, S. Mukamel, Electrostatic DFT map for the complete vibrational amide band of NMA, J. Phys. Chem., A 109 (2005) 9747–9759.
[202] W.H. Moore, S. Krimm, Transition dipole coupling in amide I modes of ß-polypeptides, Proc. Natl. Acad. Sci. U. S. A. 72 (1975) 4933–4935.

[203] H. Torii, M. Tasumi, Model calculations on the amide-I infrared bands of globular proteins, J. Chem. Phys. 96 (1992) 3379–3387.
[204] H. Torii, M. Tasumi, Theoretical analyses of the amide I infrared bands of globular proteins, in: H.H. Mantsch, D. Chapman (Eds.), Infrared Spectroscopy of Biolmolecules, Wiley-Liss, New York, 1996, pp. 1–18.
[205] T.M. Watson, J.D. Hirst, Calculating vibrational frequencies of amides: from formamide to concanavalin A, Phys. Chem. Chem. Phys. 6 (2004) 998–1005.
[206] H. Torii, M. Tasumi, Application of the three-dimensional doorway-state theory to analyses of the amide-I infrared bands of globular proteins, J. Chem. Phys. 97 (1992) 92–98.
[207] J.W. Brauner, C.R. Flach, R. Mendelsohn, A quantitative reconstruction of the amide I contour in the IR spectra of globular proteins: from structure to spectrum, J. Am. Chem. Soc. 127 (2005) 100–109.
[208] T.M. Watson, J.D. Hirst, Theoretical studies of the amide I vibrational frequencies of [Leu]-enkephalin, Mol. Phys. 103 (2005) 1531–1546.
[209] S. Ham, S. Cha, J.-H. Choi, M. Cho, Amide I modes of tripeptides: Hessian matrix reconstruction and isotope effects, J. Chem. Phys. 119 (2003) 1451–1461.
[210] S.-H. Lee, S. Krimm, General treatment of vibrations of helical molecules and application to transition dipole coupling in amide I and amide II modes of α-helical poly(L-alanine), Chem. Phys. 230 (1998) 277–295.
[211] J. Kubelka, T.A. Keiderling, The anomalous infrared amide I intensity distribution in ^{13}C isotopically labeled peptide ß-sheets comes from extended multiple-stranded structures. An ab initio study, J. Am. Chem. Soc. 123 (2001) 6142–6150.
[212] J. Kubelka, T.A. Keiderling, Differentiation of ß-sheet-forming structures: ab initio-based simulations of IR absorption and vibrational CD for model peptide and protein ß-sheets, J. Am. Chem. Soc. 123 (2001) 12048–12058.
[213] T. Heimburg, J. Schuenemann, K. Weber, N. Geisler, Specific recognition of coiled coils by infrared spectroscopy: analysis of the three structural domains of type III intermediate filament proteins, Biochemistry 35 (1996) 1375–1382.
[214] Y.N. Chirgadze, E.V. Brazhnikov, Intensities and other spectral parameters of infrared amide bands of polypeptides in the _-helical form, Biopolymers 13 (1974) 1701–1712.
[215] G. Martinez, G. Millhauser, FTIR spectroscopy of alanine-based peptides: assignment of the amide I′ modes for random coil and helix, J. Struct. Biol. 114 (1995) 23–27.
[216] S. Mukherjee, P. Chowdhury, F. Gai, Infrared study of the effect of hydration on the amide I band and aggregation properties of helical peptides, J. Phys. Chem., B 111 (2007) 4596–4602.
[217] P. Chitnumsub, W.R. Fiori, H.A. Lashuel, H. Diaz, J.W. Kelly, The nucleation of monomeric parallel ß-sheet-like structures and their self-assembly in aqueous solution, Bioorg. Med. Chem. 7 (1999) 39–59.
[218] R. Khurana, A.L. Fink, Do parallel ß-helix proteins have a unique Fourier transform infrared spectrum? Biophys. J. 78 (2000) 994–1000.
[219] N. Yamado, K. Ariga, M. Naito, K. Matsubara, E. Koyama, Regulation of ß-sheet structures within amyloid-like ß-sheets assemblage from tripeptide derivatives, J. Am. Chem. Soc. 120 (1998) 12192–12199.
[220] H. Susi, D.M. Byler, FTIR study of proteins with parallel ß chains, Arch. Biochem. Biophys. 258 (1987) 465–469.
[221] H. Susi, N. Timasheff, L. Stevens, Infrared spectra and protein conformation in aqueous solutions 1. The amide I band in H_2O and D_2O solutions, J. Biol. Chem. 242 (1967) 5460–5466.
[222] S.N. Timasheff, H. Susi, L. Stevens, Infrared spectra and protein conformations in aqueous solutions, J. Biol. Chem. 242 (1967) 5467–5473.
[223] J. Wang, M.G. Sowa, K. Ahmed, H.H. Mantsch, Photoacoustic near-infrared investigation of homo-polypeptides, J. Phys. Chem. 98 (1994) 4748–4755.
[224] M. Miyazawa, M. Sonoyama, Second derivative near infrared studies on the structural characterisation of proteins, J. Near Infrared Spectrosc. 6 (1998) A253–A257.
[225] S. Naves, A. De Juan, R. Tauler, Modeling temperature-dependent protein structural transitions by combined near-IR and mid-IR spectroscopies and multivariate curve resolution, Anal. Chem. 75 (2003) 5592–5601.
[226] P. Robert, M.F. Devaux, N. Mouhous, E. Dufour, Monitoring the secondary structure of proteins by near-infrared spectroscopy, Appl. Spectrosc. 53 (1999) 226–232.
[227] J.A. Hering, P.R. Innocent, P.I. Haris, Towards developing a protein infrared spectra databank (PISD) for proteomics research, Proteomics 4 (2004) 2310–2319.
[228] D.M. Byler, H. Susi, Examination of the secondary structure of proteins by deconvolved FTIR spectra, Biopolymers 25 (1986) 469–487.
[229] J.K. Kauppinen, D.J. Moffatt, H.H. Mantsch, D.G. Cameron, Fourier self-deconvolution: A method for resolving intrinsically overlapping bands, Appl. Spectrosc. 35 (1981) 271–276.
[230] H.H. Mantsch, D.J. Moffatt, H.L. Casal, Fourier transform methods for spectral resolution enhancement, J. Mol. Struct. 173 (1988) 285–298.
[231] H. Susi, D.M. Byler, Resolution-enhanced Fourier transform infrared spectroscopy of enzymes, Methods Enzymol. 130 (1986) 290–311.
[232] A. Barth, Fine-structure enhancement — Assessment of a simple method to resolve overlapping bands in spectra, Spectrochim. Acta, A 56 (2000) 1223–1232.
[233] R.W.J. Sarver, W.C. Krueger, Protein secondary structure from Fourier transform infrared spectroscopy: a data base analysis, Anal. Biochem. 194 (1991) 89–100.
[234] R. Pribic, I.H.M. Van Stokkum, D. Chapman, P.I. Haris, M. Bloemendal, Protein secondary structure from Fourier transform infrared and/or circular dichroism spectra, Anal. Biochem. 214 (1993) 366–378.
[235] N.N. Kalnin, I.A. Baikalov, S.Y. Venyaminov, Quantitative IR spectrophotometry of peptide compounds in Water (H_2O) solutions. III. Estimation of the protein secondary structure, Biopolymers 30 (1990) 1273–1280.
[236] F. Dousseau, M. Pezolet, Determination of the secondary structure content of proteins in aqueous solutions from their amide I and amide II infrared bands. Comparison between classical and partial least-squares methods, Biochemistry 29 (1990) 8771–8779.
[237] D.C. Lee, P.I. Haris, D. Chapman, R.C. Mitchell, Determination of protein secondary structure using factor analysis of infrared spectra, Biochemistry 29 (1990) 9185–9193.
[238] V. Baumruk, P. Pancoska, T.A. Keiderling, Predictions of secondary structure using statistical analyses of electronic and vibrational circular dichroism and Fourier transform infrared spectra of proteins in H_2O, J. Mol. Biol. 259 (1996) 774–791.
[239] J.A. Hering, P.R. Innocent, P.I. Haris, Automatic amide I frequency selection for rapid quantification of protein secondary structure from Fourier transform infrared spectra of proteins, Proteomics 2 (2002) 839–849.
[240] E. Goormaghtigh, J.-M. Ruysschaert, V. Raussens, Evaluation of the information content in infrared spectra for protein secondary structure determination, Biophys. J. 90 (2006) 2946–2957.
[241] J. Backmann, H. Fabian, D. Naumann, Temperature-jump-induced refolding of ribonuclease A: a time-resolved FTIR spectroscopic study, FEBS Lett. 364 (1995) 175–178.
[242] W.K. Surewicz, A.G. Szabo, H.H. Mantsch, Conformational properties of azurin in solution as determined from resolution-enhanced Fourier-transform infrared spectra, Eur. J. Biochem. 167 (1987) 519–523.
[243] D. Reinstädler, H. Fabian, J. Backmann, D. Naumann, Refolding of thermally and urea-denatured ribonuclease A monitored by time-resolved FTIR spectroscopy, Biochemistry 35 (1996) 15822–15830.
[244] H. Fabian, D. Naumann, Methods to study protein folding by stopped-flow FT-IR, Methods 34 (2004) 28–40.
[245] E.A. Gooding, A.P. Ramajo, J.W. Wang, C. Palmer, E. Fouts, M. Volk, The effects of individual amino acids on the fast folding dynamics of α-helical peptides, Chem. Commun. 2005 (2005) 5985–5987.
[246] S.H. Brewer, B.B. Song, D.P. Raleigh, R.B. Dyer, Residue specific resolution of protein folding dynamics using isotope-edited infrared temperature jump spectroscopy, Biochemistry 46 (2007) 3279–3285.
[247] W.K. Surewicz, J.J. Leddy, H.H. Mantsch, Structure, stability and receptor interaction of cholera toxin as studied by Fourier-transform infrared spectroscopy, Biochemistry 29 (1990) 8106–8111.

[248] M. Jackson, H.H. Mantsch, Beware of proteins in DMSO, Biochim. Biophys. Acta 1078 (1991) 231–235.
[249] M. Jackson, P.I. Haris, D. Chapman, Fourier transform infrared spectroscopic studies of Ca^{2+}-binding proteins, Biochemistry 30 (1991) 9681–9686.
[250] S.W. Englander, N.R. Kallenbach, Hydrogen exchange and structural dynamics of proteins and nucleic acids, Quart. Rev. Biophys. 4 (1984) 521–655.
[251] T.M. Raschke, S. Marqusee, Hydrogen exchange studies of protein structure, Curr. Opin. Biotechnol. 9 (1998) 80–86.
[252] E. Goormaghtigh, H.H.J. deJongh, J.M. Ruysschaert, Relevance of protein thin films prepared for attenuated total reflection Fourier transform infrared spectroscopy: Significance of the pH, Appl. Spectrosc. 50 (1996) 1519–1527.
[253] J. Le Coutre, L.R. Narasimhan, C.K.N. Patel, H.R. Kaback, The lipid bilayer determines helical tilt angle and function in lactose permease of *Escherichia coli*, Proc. Natl. Acad. Sci. U. S. A. 94 (1997) 10167–10171.
[254] J. Le Coutre, H.R. Kaback, C.K.N. Patel, L. Heginbotham, C. Miller, Fourier transform infrared spectroscopy reveals a rigid α-helical assembly for the tetrameric *Streptomyces lividans* K^+ channel, Proc. Natl. Acad. Sci. U. S. A. 95 (1998) 6114–6117.
[255] N.W. Downer, T.J. Bruchman, J.H. Hazzard, Infrared spectroscopic study of photoreceptor membrane and purple membrane, J. Biol. Chem. 261 (1986) 3640–3647.
[256] T.N. Earnest, J. Herzfeld, K.J. Rothschild, Polarized Fourier-transform infrared-spectroscopy of bacteriorhodopsin—transmembrane alpha-helices are resistant to hydrogen–deuterium exchange, Biophys. J. 58 (1990) 1539–1546.
[257] F. Scheirlinckx, R. Buchet, J.-M. Ruysschaert, E. Goormaghtigh, Monitoring of secondary and tertiary structure changes in the gastric H^+/K^+-ATPase by infrared spectroscopy, Eur. J. Biochem. 268 (2001) 3644–3653.
[258] E. Goormaghtigh, L. Vigneron, G.A. Scarborough, J.-M. Ruysschaert, Tertiary conformational changes of the *Neurospora crassa* plasma membrane H^+-ATPase monitored by hydrogen/deuterium exchange kinetics, J. Biol. Chem. 269 (1994) 27409–27413.
[259] C. Vigano, A. Margolles, H.W. van Veen, W.N. Konings, J.-M. Ruysschaert, Secondary and tertiary structure changes of reconstituted LmrA induced by nucleotide binding or hydrolysis, J. Biol. Chem. 275 (2000) 10962–10967.
[260] A. Muga, H.H. Mantsch, W.K. Surewicz, Membrane-binding induces destabilization of cytochrome-c structure, Biochemistry 30 (1991) 7219–7224.
[261] F. Scheirlinckx, V. Raussens, J.-M. Ruysschaert, E. Goormaghtigh, Conformational changes in gastric H^+/K^+-ATPase monitored by difference Fourier-transform infrared spectroscopy and hydrogen/deuterium exchange, Biochem. J. 382 (2004) 121–129.
[262] J. Trewhalla, W.K. Liddle, D.B. Heidorn, N. Strynadka, Calmodulin and troponin C structures studied by Fourier transform infrared spectroscopy: Effects of calcium and magnesium binding, Biochemistry 28 (1989) 1294–1301.
[263] H. Fabian, T. Yuan, H.J. Vogel, H.H. Mantsch, Comparative analysis of the amino- and carboxy-terminal domains of calmodulin by Fourier transform infrared spectroscopy, Eur. Biophys. J. 24 (1996) 195–201.
[264] J.O. Alben, W.S. Caughey, An infrared study of bound carbon monoxide in the human red blood cell, isolated hemoglobin, and heme carbonyls, Biochemistry 7 (1968) 175–183.
[265] M.E. Riepe, J.H. Wang, Infrared studies on the mechanism of action of carbonic anhydrase, J. Biol. Chem. 243 (1968) 2779–2787.
[266] J.G. Belasco, J.R. Knowles, Direct observation of substrate distortion by triosephosphate isomerase using Fourier transform infrared spectroscopy, Biochemistry 19 (1980) 472–477.
[267] P. Tonge, G.R. Moore, C.W. Wharton, Fourier-transform infra-red studies of the alkaline isomerization of mitochondrial cytochrome *c* and the ionization of carboxylic acids, Biochem. J. 258 (1989) 599–605.
[268] P.J. Tonge, M. Pusztai, A.J. White, C.W. Wharton, P.R. Carey, Resonance Raman and Fourier transform infrared spectroscopic studies of the acyl carbonyl group in [3-(5-methyl-2-thienyl)acryloyl]chymotrypsin: evidence for artefacts in the spectra obtained by both techniques, Biochemistry 30 (1991) 4790–4795.
[269] G. Zundel, Hydrogen bonds with large proton polarizability and proton transfer processes in electrochemistry and biology, Adv. Chem. Phys. 111 (2000) 1–217.
[270] G. Iliadis, G. Zundel, B. Brzezinski, Catalytic mechanism of the aspartate proteinase pepsin A: an FTIR study, Biospectroscopy 3 (1997) 291–297.
[271] F. Bartl, D. Palm, R. Schinzel, G. Zundel, Proton relay system in the active site of maltodextrinphosphorylase via hydrogen bonds with large proton polarizability: an FT-IR difference spectroscopy study, Eur. Biophys. J. 28 (1999) 200–207.
[272] M. Steiner, H. Bauer, F. Krassnigg, W.-B. Schill, H. Adam, Micromethod for determination of ATPase activities using bioluminescence technique, Clin. Chem. Acta 177 (1988) 107–114.
[273] R. Pacheco, A. Karmali, M.L.M. Serralheiro, P.I. Haris, Application of Fourier transform infrared spectroscopy for monitoring hydrolysis and synthesis reactions catalyzed by a recombinant amidase, Anal. Biochem. 346 (2005) 49–58.
[274] W.A.P. Luck, The importance of cooperativity for the properties of liquid water, J. Mol. Struct. 448 (1998) 131–142.
[275] J.M. Vanderkooi, J.L. Dashnau, B. Zelent, Temperature excursion infrared (TEIR) spectroscopy used to study hydrogen bonding between water and biomolecules, Biochim. Biophys. Acta 1749 (2005) 214–233.
[276] Y. Maréchal, Observing the water molecule in macromolecules and aqueous media using infrared spectrometry, J. Mol. Struct. 648 (2003) 27–47.
[277] U. Buck, F. Huisken, Infrared spectroscopy of size-selected water and methanol clusters, Chem. Rev. 100 (2000) 3863–3890.
[278] J.A. Rupley, G. Careri, Protein hydration and function, Adv. Prot. Chem. 41 (1991) 37–172.
[279] K. Liltorp, Y. Maréchal, Hydration of lysozyme as observed by infrared spectrometry, Biopolymers 79 (2005) 185–196.
[280] J. Grdadolnik, Y. Maréchal, Bovine serum albumin observed by infrared spectrometry. II. Hydration mechanisms and interaction configurations of embedded H_2O molecules, Biopolymers (Biospectroscopy) 62 (2000) 54–67.
[281] M. Leonhard, W. Mäntele, Fourier transform infrared spectroscopy and electrochemistry of the primary electron donor in *Rhodobacter sphaeroides* and *Rhodopseudomonas viridis* reaction centers: vibrational modes of the pigments in situ and evidence for protein and water modes affected by P^+ formation, Biochemistry 32 (1993) 4532–4538.
[282] A. Maeda, F.L. Tomson, R.B. Gennis, H. Kandori, T.G. Ebrey, S.P. Balashov, Relocation of internal bound water in bacteriorhodopsin during the photoreaction of M at low temperatures: an FTIR study, Biochemistry 39 (2000) 10154–10162.
[283] A. Maeda, Internal water molecules as mobile polar groups for light-induced proton translocation in bacteriorhodopsin and rhodopsin as studied by difference FTIR spectroscopy, Biochemistry (Moscow) 66 (2001) 1256–1268.
[284] H. Kandori, Role of internal water molecules in bacteriorhodopsin, Biochim. Biophys. Acta 1460 (2000) 177–191.
[285] M. Shibata, T. Tanimoto, H. Kandori, Water molecules in the Schiff base region of bacteriorhodopsin, J. Am. Chem. Soc. 125 (2003) 13312–13313.
[286] F. Garczarek, K. Gerwert, Functional waters in intraprotein proton transfer monitored by FTIR difference spectroscopy, Nature 439 (2006) 109–112.
[287] W.B. Fischer, S. Sonar, T. Marti, H.G. Khorana, K.J. Rothschild, Detection of a water molecule in the active-site of bacteriorhodopsin — hydrogen bonding changes during the primary photoreaction, Biochemistry 33 (1994) 12757–12762.
[288] Y. Furutani, A.G. Bezerra Jr., S. Waschuk, M. Sumii, L.S. Brown, H. Kandori, FTIR spectroscopy of the K photointermediate of *Neurospora* Rhodopsin: structural changes of the retinal, protein, and water molecules after photoisomerization, Biochemistry 43 (2004) 9636–9646.
[289] Y. Furutani, A. Kawanabe, K.-H. Jung, H. Kandori, FTIR spectroscopy of the all-trans form of *Anabaena* sensory rhodopsin at 77 K: hydrogen bond of a water between the Schiff base and Asp75, Biochemistry 44 (2005) 12287–12296.

[290] T. Noguchi, M. Sugiura, Structure of an active water molecule in the water-oxidizing complex of photosystem II as studied by FTIR spectroscopy, Biochemistry 39 (2000) 10943–10949.
[291] E.A. Gorbikova, N.P. Belevich, M. Wikström, M.I. Verkhovsky, Protolytic reactions on reduction of cytochrome *c* oxidase studied by ATR-FTIR spectroscopy, Biochemistry 46 (2007) 4177–4183.
[292] P.E. Fraley, K.N. Rao, High resolution infrared spectra of water vapor. ν_1 and ν_3 band of $H_2^{16}O$, J. Mol. Spectrosc. 29 (1969) 348–364.
[293] B. Rowland, J.P. Devlin, Spectra of dangling OH groups at ice cluster surfaces and within pores of amorphous ice, J. Chem. Phys. 94 (1991) 812–813.
[294] X. Wei, P.B. Miranda, C. Zhang, Y.R. Shen, Sum-frequency spectroscopic studies of ice interfaces, Phys. Rev., B 66 (2002) 085401.
[295] K. Ohno, M. Okimura, N. Akai, Y. Katsumoto, The effect of cooperative hydrogen bonding on the OH stretching-band shift for water clusters studied by matrix-isolation infrared spectroscopy and density functional theory, Phys. Chem. Chem. Phys. 7 (2005) 3005–3014.
[296] Q. Du, R. Superfine, E. Freysz, Y.R. Shen, Vibrational spectroscopy of water at the vapor/water interface, Phys. Rev. Lett. 70 (1993) 2313–2316.
[297] J.M. Headrick, E.G. Diken, R.S. Walters, N.I. Hammer, R.A. Christie, J. Cui, E.M. Myshakin, M.A. Duncan, M.A. Johnson, K.D. Jordan, Spectral signatures of hydrated proton vibrations in water clusters, Science 308 (2005) 1765–1769.
[298] H.A. Schwarz, Gas phase infrared spectra of oxonium hydrate ions from 2 to 5 μ, J. Chem. Phys. 67 (1977) 5525–5534.
[299] K.R. Asmis, N.L. Pivonka, G. Santambrogio, M. Brümmer, C. Kaposta, D.M. Neumark, L. Wöste, Gas-phase infrared spectrum of the protonated water dimer, Science 299 (2003) 1375–1377.
[300] M. Falk, P.A. Giguere, Infrared spectrum of the H_3O^+ ion in aqueous solutions, Can. J. Chem. 35 (1957) 1195–1204.
[301] N.B. Librovich, V.P. Sakun, N.D. Sokolov, H^+ and OH^- ions in aqueous solutions. Vibrational spectra of hydrates, Chem. Phys. 39 (1979) 351–366.
[302] J. Breton, E. Nabedryk, Proton uptake upon quinone reduction in bacterial reaction centers: IR signature and possible participation of a highly polarizable hydrogen bond network, Photosynth. Res. 55 (1998) 301–307.
[303] J. Kim, U.W. Schmitt, J.A. Gruetzmacher, G.A. Voth, N.E. Scherer, The vibrational spectrum of the hydrated proton: Comparison of experiment, simulation, and normal mode analysis, J. Chem. Phys. 116 (2002) 737–746.
[304] J. Riesle, D. Oesterhelt, N.A. Dencher, J. Heberle, D38 is an essential part of the proton translocation pathway in bacteriorhodopsin, Biochemistry 35 (1996) 6635–6643.
[305] R. Rammelsberg, G. Huhn, M. Lübben, K. Gerwert, Bacteriorhodopsin's intramolecular proton-release pathway consists of a hydrogen-bonded network, Biochemistry 37 (1998) 5001–5009.
[306] J. Wang, M.A. El-Sayed, Time-resolved Fourier transform infrared spectroscopy of the polarizable proton continua and the proton pump mechanism of bacteriorhodopsin, Biophys. J. 80 (2001) 961–971.
[307] F. Garczarek, L.S. Brown, J.K. Lanyi, K. Gerwert, Proton binding within a membrane protein by a protonated water cluster, Proc. Natl. Acad. Sci. U. S. A. 102 (2005) 3633–3638.
[308] R. Rousseau, V. Kleinschmidt, U.W. Schmitt, D. Marx, Assigning protonation patterns in water networks in bacteriorhodopsin based on computed IR spectra, Angew. Chem. Int. Ed. 43 (2004) 4804–4807.
[309] J.E. Baenziger, K.W. Miller, K.J. Rothschild, Fourier transform infrared difference spectroscopy of the nicotinic acetylcholine receptor: evidence for specific protein structural changes upon desensitization, Biochemistry 32 (1993) 5448.
[310] J.E. Baenziger, K.W. Miller, K.J. Rothschild, Incorporation of the nicotinic acetylcholine receptor into planar multilamellar films: characterization by fluorescence and Fourier transform infrared difference spectroscopy, Biophys. J. 61 (1992) 983–992.
[311] J.H. Kaplan, B. Forbush, J.F. Hoffman, Rapid photolytic release of ATP from a protected analogue: utilization by the Na:K pump of human red blood cell ghosts, Biochemistry 17 (1978) 1929–1935.
[312] J.A. McCray, L. Herbette, T. Kihara, D.R. Trentham, A new approach to time-resolved studies of ATP-requiring biological systems: Laser flash photolysis of caged ATP, Proc. Natl. Acad. Sci. U. S. A. 77 (1980) 7237–7241.
[313] J.A. McCray, D.R. Trentham, Properties and uses of photoreactive caged compounds, Annu. Rev. Biophys. Biophys. Chem. 18 (1989) 239–270.
[314] J.E.T. Corrie, D.R. Trentham, Caged nucleotides and neurotransmitters, in: H. Morrison (Ed.), Bioorganic Photochemistry, Vol. 2, John Wiley & Sons, New York, 1993, pp. 243–305.
[315] J.M. Nerbonne, Design and application of photolabile intracellular probes, in: P. De Weer, B. Salzberg (Eds.), Optical Methods in Cell Physiology, Wiley, New York, 1986, pp. 417–445.
[316] H.A. Lester, J.M. Nerbonne, Physiological and pharmacological manipulations with light flashes, Annu. Rev. Biophys. Bioeng. 11 (1982) 151–175.
[317] A.M. Gurney, H.A. Lester, Light-flash physiology with synthetic photosensitive compounds, Physiol. Rev. 67 (1987) 583–617.
[318] A. Barth, W. Mäntele, W. Kreutz, Molecular changes in the sarcoplasmic reticulum Ca^{2+} ATPase during catalytic activity. A Fourier transform infrared (FTIR) study using photolysis of caged ATP to trigger the reaction cycle, FEBS Lett. 277 (1990) 147–150.
[319] A. Barth, K. Hauser, W. Mäntele, J.E.T. Corrie, D.R. Trentham, Photochemical release of ATP from 'caged ATP' studied by time-resolved infrared spectroscopy, J. Am. Chem. Soc. 117 (1995) 10311–10316.
[320] A. Barth, J.E.T. Corrie, M.J. Gradwell, Y. Maeda, W. Mäntele, T. Meier, D.R. Trentham, Time-resolved infrared spectroscopy of intermediates and products from photolysis of 1-(2-nitrophenyl)ethyl phosphates: reaction of the 2-nitrosoacetophenone byproduct with thiols, J. Am. Chem. Soc. 119 (1997) 4149–4159.
[321] V. Cepus, C. Ulbrich, C. Allin, A. Troullier, K. Gerwert, Fourier transform infrared photolysis studies of caged compounds, Methods Enzymol. 291 (1998) 223–245.
[322] A. Barth, Time-resolved IR spectroscopy with caged compounds: An introduction, in: M. Goeldner, R.S. Givens (Eds.), Dynamic Studies in Biology: Phototriggers, Photoswitches and Caged Biomolecules, Wiley-VCH, Weinheim, 2005.
[323] M. Liu, E.-L. Karjalainen, A. Barth, Use of helper enzymes for ADP removal in infrared spectroscopic experiments: application to Ca^{2+}-ATPase, Biophys. J. 88 (2005) 3615–3624.
[324] S. Williams, T.P. Causgrove, R. Gilmanshin, K.S. Fang, R.H. Callender, W.H. Woodruff, R.B. Dyer, Fast events in protein folding: Helix melting and formation in a small peptide, Biochemistry 35 (1996) 691–697.
[325] J. Wang, M.A. El-Sayed, Temperature jump-induced secondary structural change of the membrane protein bacteriorhodopsin in the premelting temperature region: a nanosecond time-resolved Fourier transform infrared study, Biophys. J. 76 (1999) 2777–2783.
[326] C.M. Phillips, Y. Mizutani, R.M. Hochstrasser, Ultrafast thermally induced unfolding of RNase A, Proc. Natl. Acad. Sci. U. S. A. 92 (1995) 7292–7296.
[327] A.P. Ramajo, S.A. Petty, M. Volk, Fast folding dynamics of α-helical peptides — Effect of solvent additives and pH, Chem. Phys. 323 (2006) 11–20.
[328] G. Panick, R. Malessa, R. Winter, G. Rapp, K.J. Frye, C.A. Royer, Structural characterization of the pressure-denatured state and unfolding/refolding kinetics of staphylococcal nuclease by synchrotron small-angle X-ray scattering and Fourier-transform infrared spectroscopy, J. Mol. Biol. 275 (1998) 389–402.
[329] G. Panick, R. Winter, Pressure-induced unfolding/refolding of ribonuclease A: static and kinetic Fourier transform infrared spectroscopy study, Biochemistry 39 (2000) 1862–1869.
[330] D. Moss, E. Nabedryk, J. Breton, W. Mäntele, Redox-linked conformational changes in proteins detected by a combination of infrared spectroscopy and protein electrochemistry. Evaluation of the technique with cytochrome *c*, Eur. J. Biochem. 187 (1990) 565–572.
[331] M. Bauscher, M. Leonhard, D.A. Moss, W. Mäntele, Binding and interaction of the primary and the secondary electron acceptor quinones in bacterial photosynthesis. An infrared spectroelectrochemical study of *Rhodobacter sphaeroides* reaction centers, Biochim. Biophys. Acta 1183 (1993) 59–71.

[332] E. Hamacher, J. Kruip, M. Rögner, W. Mäntele, Characterization of the primary electron donor of photosystem I, P700, by electrochemistry and Fourier transform infrared (FTIR) difference spectroscopy, Spectrochim. Acta, A 52 (1996) 107–121.
[333] P. Hellwig, J. Behr, C. Ostermeier, O.M. Richter, U. Pfitzner, A. Odenwald, B. Ludwig, H. Michel, W. Mäntele, Involvement of glutamic acid 278 in the redox reaction of the cytochrome *c* oxidase from *Paracoccus denitrificans* investigated by FTIR spectroscopy, Biochemistry 37 (1998) 7390–7399.
[334] P. Hellwig, B. Rost, U. Kaiser, C. Ostermeier, H. Michel, W. Mäntele, Carboxyl group protonation upon reduction of the *Paracoccus denitrificans* cytochrome *c* oxidase: direct evidence by FTIR spectroscopy, FEBS Lett. 385 (1996) 53–57.
[335] J. Behr, P. Hellwig, W. Mäntele, H. Michel, Redox dependent changes at the heme propionates in cytochrome *c* oxidase from *Paracoccus denitrificans:* direct evidence from FTIR difference spectroscopy in combination with heme propionate ^{13}C labeling, Biochemistry 37 (1998) 7400–7406.
[336] P. Hellwig, C. Ostermeier, H. Michel, B. Ludwig, W. Mäntele, Electrochemically induced FT-IR difference spectra of the two- and four-subunit cytochrome *c* oxidase from *P. denitrificans* reveal identical conformational changes upon redox transitions, Biochim. Biophys. Acta 1409 (1998) 107–112.
[337] P. Hellwig, T. Soulimane, G. Buse, W. Mäntele, Similarities and dissimilarities in the structure–function relation between the cytochrome *c* oxidase from bovine heart and from *Paracoccus denitrificans* as revealed by FT-IR difference spectroscopy, FEBS Lett. 458 (1999) 83–86.
[338] B. Rost, J. Behr, P. Hellwig, O.M. Richter, B. Ludwig, H. Michel, W. Mäntele, Time-resolved FT-IR studies on the CO adduct of *Paracoccus denitrificans* cytochrome *c* oxidase: comparison of the fully reduced and the mixed valence form, Biochemistry 38 (1999) 7565–7571.
[339] J. Behr, H. Michel, W. Mäntele, P. Hellwig, Functional properties of the heme propionates in cytochrome *c* oxidase from *Paracoccus denitrificans*. Evidence from FTIR difference spectroscopy and site-directed mutagenesis, Biochemistry 39 (2000) 1356–1363.
[340] E.D. Dodson, X.J. Zhao, W.S. Caughey, C.M. Elliott, Redox dependent interactions of the metal sites in carbon monoxide-bound cytochrome C oxidase monitored by infrared and UV/visible spectroelectrochemical methods, Biochemistry 35 (1996) 444–452.
[341] G. Tollin, Use of flavin photochemistry to probe intraprotein and inter protein electron transfer mechanisms, J. Bioenerg. Biomembr. 27 (1995) 303–309.
[342] R. Traber, H.E.A. Kramer, P. Hemmerich, Mechanism of light-induced reduction of biological redox centers by amino acids. A flash photolysis study of flavin photoreduction by ethylenediaminetetraacetate and nitrilotriacetate, Biochemistry 21 (1982) 1687–1693.
[343] J. Contzen, C. Jung, Changes in secondary structure and salt links of cytochrome P-450cam induced by photoreduction: A Fourier transform infrared spectroscopic study, Biochemistry 38 (1999) 16253–16260.
[344] M. Lübben, K. Gerwert, Redox FTIR difference spectroscopy using caged electrons reveals contributions of carboxyl groups to the catalytic mechanism of haem-copper oxidases, FEBS Lett. 397 (1996) 303–307.
[345] M. Lübben, A. Prutsch, B. Mamat, K. Gerwert, Electron transfer induces side-chain conformational changes of glutamate-286 from cytochrome bo_3, Biochemistry 38 (1999) 2048–2056.
[346] Y. Yamazaki, H. Kandori, T. Mogi, Effects of subunit I mutations on redox-linked conformational changes of the *Escherichia coli bo*-type ubiquinol oxidase revealed by Fourier-transform infrared spectroscopy, J. Biochem. 126 (1999) 194–199.
[347] Y. Yamazaki, H. Kandori, T. Mogi, Fourier-transform infrared studies on conformation changes in *bd*-type ubiquinol oxidase from *Escherichia coli* upon photoreduction of the redox metal centers, J. Biochem. 125 (1999) 1131–1136.
[348] M. Liu, A. Barth, Mapping interactions between the Ca^{2+}-ATPase and its substrate ATP with infrared spectroscopy, J. Biol. Chem. 278 (2003) 10112–10118.
[349] A. Barth, F. von Germar, W. Kreutz, W. Mäntele, Time-resolved infrared spectroscopy of the Ca^{2+}-ATPase. The enzyme at work, J. Biol. Chem. 271 (1996) 30637–30646.
[350] R. Brudler, R. Rammelsberg, T.T. Woo, E.D. Getzoff, K. Gerwert, Structure of the I_1 early intermediate of photoactive yellow protein by FTIR spectroscopy, Nat. Struct. Biol. 8 (2001) 265–270.
[351] R.S. Chittock, S. Ward, A.-S. Wilkinson, P. Caspers, B. Mensch, M.G.P. Page, C.W. Wharton, Hydrogen bonding and protein perturbation in ß-lactam acyl-enzymes of *streptococcus pneumoniae* penicilin-binding protein PBP2x, Biochem. J. 338 (1999) 153–159.
[352] A. Troullier, K. Gerwert, Y. Dupont, A time-resolved Fourier transformed infrared difference spectroscopy study of the sarcoplasmic reticulum Ca^{2+}-ATPase: kinetics of the high-affinity calcium binding at low temperature, Biophys. J. 71 (1996) 2970–2983.
[353] M. Liu, A. Barth, Phosphorylation of the sarcoplasmic reticulum Ca^{2+}-ATPase from ATP and ATP analogs studied by infrared spectroscopy, J. Biol. Chem. 279 (2004) 49902–49909.
[354] J.J. Katz, L.L. Shipman, T.M. Cotton, T.R. Janson, Chlorophyll aggregation: coordination interactions in chlorophyll monomers, dimers, and oligomers, in: D. Dolphin (Ed.), The Porphins, vol. 5, Academic Press, New York, 1978, pp. 401–458.
[355] J.J. Katz, R.C. Dougherty, L.J. Boucher, Infrared and nuclear magnetic resonance spectroscopy of chlorophyll, in: L.P. Vernon, G.R. Seely (Eds.), The Chlorophylls, Academic Press, New York, 1966, pp. 185–251.
[356] M. Lutz, W. Mäntele, Vibrational spectroscopy of chlorophylls, in: H. Scheer (Ed.), Chlorophylls, CRC Press, Boca Raton, Florida, 1991, pp. 855–902.
[357] W.T. Potter, M.P. Tucker, R.A. Houtchens, W.S. Caughey, Oxygen infrared spectra of oxyhemoglobins and oxymyoglobins. Evidence of two major liganded O_2 structures, Biochemistry 26 (1987) 4699–4707.
[358] P.K. Slaich, W.U. Primrose, D.H. Robinson, C.W. Wharton, A.J. White, K. Drabble, G.C.K. Roberts, The binding of amide substrate analogues to phospholipase A_2, Biochem. J. 288 (1992) 167–173.
[359] X. Du, H. Frei, S.-H. Kim, The mechanism of GTP hydrolysis by ras probed by Fourier transform infrared spectroscopy, J. Biol. Chem. 275 (2000) 8492–8500.
[360] C. Allin, K. Gerwert, Ras catalyzes GTP hydrolysis by shifting negative charges from γ- to ß-phosphate as revealed by time-resolved FTIR difference spectroscopy, Biochemistry 40 (2001) 3037–3046.
[361] M. Liu, M. Krasteva, A. Barth, Interactions of phosphate groups of ATP and aspartyl phosphate with the sarcoplasmic reticulum Ca^{2+}-ATPase. An FTIR study, Biophys. J. 89 (2005) 4352–4363.
[362] K. Gerwert, F. Siebert, Evidence for light-induced 13-cis, 14-s-cis isomerization in bacteriorhodopsin obtained by FTIR difference spectroscopy using isotopically labeled retinals, EMBO J. 5 (1986) 805–811.
[363] P.I. Haris, G.T. Robillard, A.A. Van Dijk, D. Chapman, Potential of ^{13}C and ^{15}N labeling for studying protein–protein interactions using Fourier transform infrared spectroscopy, Biochemistry 31 (1992) 6279–6284.
[364] S. Sonar, C.P. Lee, M. Coleman, N. Patel, X. Liu, T. Marti, H.G. Khorana, U.L. RajBhandary, K.J. Rothschild, Site-directed isotope labeling and FTIR spectroscopy of bacteriorhodopsin, Struct. Biol. 1 (1994) 512–517.
[365] J.L. Spudich, New tool for spectroscopists, Struct. Biol. 1 (1994) 495–496.
[366] H. Fabian, D. Chapman, H.H. Mantsch, New trends in isotope-edited infrared spectroscopy, in: H.H. Mantsch, D. Chapman (Eds.), Infrared Spectroscopy of Biomolecules, Wiley-Liss, New York, 1996, pp. 341–352.
[367] S.M. Decatur, Elucidation of residue-level structure and dynamics of polypeptides via isotope-edited infrared spectroscopy, Acc. Chem. Res. 39 (2006) 169–175.
[368] I.T. Arkin, Isotope-edited IR spectroscopy for the study of membrane proteins, Curr. Opin. Chem. Biol. 10 (2006) 394–401.
[369] K.P. Das, L.P. Choo-Smith, J.M. Petrash, W.K. Surewicz, Insight into the secondary structure of non-native proteins bound to a molecular chaperone α-crystallin—An isotope-edited infrared spectroscopic study, J. Biol. Chem. 274 (1999) 33209–33212.
[370] M. Zhang, H. Fabian, H.H. Mantsch, H.J. Vogel, Isotope-edited Fourier

transform infrared spectroscopy studies of calmodulin's interaction with its target peptides, Biochemistry 33 (1994) 10883–10888.
[371] C.F.C. Ludlam, I.T. Arkin, X.M. Liu, M.S. Rothman, P. Rath, S. Aimoto, S.O. Smith, D.M. Engelman, K.J. Rothschild, Fourier transform infrared spectroscopy and site-directed isotope labeling as a probe of local secondary structure in the transmembrane domain of phospholamban, Biophys. J. 70 (1996) 1728–1736.
[372] S.M. Decatur, J. Antonic, Isotope-edited infrared spectroscopy of helical peptides, J. Am. Chem. Soc. 121 (1999) 11914–11915.
[373] R.A.G.D. Silva, J. Kubelka, P. Bour, S.M. Decatur, T.A. Keiderling, Site-specific conformational determination in thermal unfolding studies of helical peptides using vibrational circular dichroism with isotopic substitution, Proc. Natl. Acad. Sci. U. S. A. 97 (2000) 8318–8323.
[374] L.M. Gordon, K.Y.C. Lee, M.M. Lipp, J.A. Zasadzinski, F.J. Walther, M.A. Sherman, A.J. Waring, Conformational mapping of the N-terminal segment of surfactant protein B in lipid using ^{13}C-enhanced Fourier transform infrared spectroscopy, J. Peptide Res. 55 (2000) 330–347.
[375] P.T. Lansbury, P.R. Costa, J.M. Griffiths, E.J. Simon, M. Auger, K.J. Halverson, D.A. Kocisko, Z.S. Hendsch, T.T. Ashburn, R.G.S. Spencer, B. Tidor, R.G. Griffin, Structural model for the ß-amyloid fibril based on interstrand alignment of an antiparallel-sheet comprising a C-terminal peptide, Nat. Struct. Biol. 2 (1995) 990–998.
[376] K.J. Rothschild, M. Zagaeski, W.A. Cantore, Conformational changes of bacteriorhodopsin detected by Fourier transform infrared difference spectroscopy, Biochem. Biophys. Res. Commun. 103 (1981) 483–489.
[377] W. Mäntele, F. Siebert, W. Kreutz, Kinetic properties of rhodopsin and bacteriorhodopsin measured by kinetic infrared spectroscopy (KIS), Methods Enzymol. 88 (1982) 729–740.
[378] F. Siebert, W. Mäntele, W. Kreutz, Evidence for the protonation of two internal carboxylic groups during the photocycle of bacteriorhodopsin, FEBS Lett. 141 (1982) 82–87.
[379] J. Sasaki, A. Maeda, C. Kato, H. Hamaguchi, Time-resolved infrared spectral analysis of the KL-to-L conversion in the photocycle of bacteriorhodopsin, Biochemistry 32 (1993) 867–871.
[380] M.S. Braiman, O. Bousché, K.J. Rothschild, Protein dynamics in the bacteriorhodopsin photocycle: submillisecond Fourier transform infrared spectra of the L, M, and N photointermediates, Proc. Natl. Acad. Sci. U. S. A. 88 (1991) 2388–2392.
[381] G. Souvignier, K. Gerwert, Proton uptake mechanism of bacteriorhodopsin as determined by time-resolved stroboscopic-FTIR-spectroscopy, Biophys. J. 63 (1992) 1393–1405.
[382] O. Weidlich, F. Siebert, Time-resolved step-scan FT-IR investigations of the transition from KL to L in the bacteriorhodopsin photocycle: identification of chromophore twists by bending vibrations, Appl. Spectrosc. 47 (1993) 1394–1400.
[383] R. Rammelsberg, B. Heßling, H. Chorongiewski, K. Gerwert, Molecular reaction mechanisms of proteins monitored by nanosecond step-scan FT-IR difference spectroscopy, Appl. Spectrosc. 51 (1997) 558–562.
[384] M. Engelhard, K. Gerwert, B. Hess, W. Kreutz, F. Siebert, Light-driven protonation changes of internal aspartic acids of bacteriorhodopsin: an investigation by static and time-resolved infrared difference spectroscopy using [4-^{13}C]aspartic acid labeled purple membrane, Biochemistry 24 (1985) 400–407.
[385] K. Fahmy, O. Weidlich, M. Engelhard, J. Tittor, D. Oesterhelt, F. Siebert, Identification of the proton acceptor of Schiff-base deprotonation in bacteriorhodopsin — a Fourier-transform-infrared study of the mutant Asp85→Glu in its natural lipid environment, Photochem. Photobiol. 56 (1992) 1073–1083.
[386] A. Maeda, J. Sasaki, Y. Shichida, T. Yoshizawa, M. Chang, B. Ni, R. Needleman, J.K. Lanyi, Structures of aspartic acid-96 in the L and N intermediates of bacteriorhodopsin: analysis by Fourier transform infrared spectroscopy, Biochemistry 31 (1992) 4684–4690.
[387] M.S. Braiman, T. Mogi, T. Marti, L.J. Stern, H.G. Khorana, K.J. Rothschild, Vibrational spectroscopy of bacteriorhodopsin mutants: light-driven proton transport involves protonation changes of aspartic acid residues 85, 96, and 212, Biochemistry 27 (1988) 8516–8520.
[388] K. Gerwert, B. Hess, J. Soppa, D. Oesterhelt, Role of aspartate-96 in proton translocation by bacteriorhodopsin, Proc. Natl. Acad. Sci. U. S. A. 86 (1989) 4943–4947.
[389] W. Kühlbrandt, Bacteriorhodopsin—The movie, Nature 406 (2000) 569–570.
[390] J.K. Lanyi, B. Schobert, Structural changes in the L photointermediate of bacteriorhodopsin, J. Mol. Biol. 365 (2007) 1379–1392.
[391] F. Siebert, W. Mäntele, Investigation of the primary photochemistry of bacteriorhodopsin by low-temperature Fourier-transform infrared spectroscopy, Eur. J. Biochem. 130 (1983) 565–573.
[392] K. Fahmy, F. Siebert, M.F. Großjean, P. Tavan, Photoisomerization in bacteriorhodopsin studied by FTIR linear dichroism and photoselection experiments combined with quantum chemical theoretical analysis, J. Mol. Struct. 214 (1989) 257–288.
[393] K. Fahmy, F. Siebert, P. Tavan, Structural investigation of bacteriorhodopsin and some of its photoproducts by polarized Fourier transform infrared spectroscopic methods — difference spectroscopy and photoselection, Biophys. J. 60 (1991) 989–1001.
[394] A. Perálvarez-Marín, V.A. Lórenz-Fonfría, J.-L. Bourdelande, E. Querol, H. Kandori, E. Padrós, Inter-helical hydrogen bonds are essential elements for intra-protein signal transduction: the role of Asp115 in bacteriorhodopsin transport function, J. Mol. Biol. 368 (2007) 666–676.
[395] G. Zundel, Hydrogen-bonded chains with large proton polarizability as charge conductors in proteins bacteriorhodopsin and the F_0 subunit of *E. coli*, J. Mol. Struct. 322 (1994) 33–42.
[396] K. Gerwert, G. Souvignier, B. Hess, Simultaneous monitoring of light-induced changes in protein side-group protonation, chromophore isomerization, and backbone motion of bacteriorhodopsin by time-resolved Fourier-transform infrared spectroscopy, Proc. Natl. Acad. Sci. U. S. A. 87 (1990) 9774–9778.
[397] M.S. Braiman, A.K. Dioumaev, J.R. Lewis, A large photolysis-induced pK_a increase of the chromophore counterion in bacteriorhodopsin: implications for ion transport mechanisms of retinal proteins, Biophys. J. 70 (1996) 939–947.
[398] Y. Cao, G. Váró, A.L. Klinger, D.M. Czaijkowsky, M.S. Braiman, R. Needleman, J.K. Lanyi, Proton transfer from Asp-96 to the bacteriorhodopsin Schiff base is caused by a decrease of the pK_a of Asp-96 which follows a protein backbone conformation change, Biochemistry 32 (1993) 1981–1990.
[399] S. Száraz, D. Oesterhelt, P. Ormos, pH-induced structural changes in bacteriorhodopsin studied by Fourier transform infrared spectroscopy, Biophys. J. 67 (1994) 1706–1712.
[400] A.K. Dioumaev, L.S. Brown, R. Needleman, J.K. Lanyi, Fourier transform infrared spectra of the late intermediate of the bacteriorhodopsin photocycle suggest transient protonation of Asp-212, Biochemistry 38 (1999) 10070–10078.
[401] C. Zscherp, R. Schlesinger, J. Heberle, Time-resolved FT-IR spectroscopic investigation of the pH-dependent proton transfer reactions in the E194Q mutant of bacteriorhodopsin, Biochem. Biophys. Res. Commun. 283 (2001) 57–63.
[402] J.O. Alben, P.P. Moh, F.G. Fiamingo, R.A. Altschuld, Cytochrome oxidase (a_3) heme and copper observed by low-temperature Fourier transform infrared spectroscopy of the CO complex, Proc. Natl. Acad. Sci. U. S. A. 78 (1981) 234–237.
[403] R.M. Nyquist, D. Heitbrink, C. Bolwien, T.A. Wells, R.B. Gennis, J. Heberle, Perfusion-induced redox differences in cytochrome *c* oxidase: ATR/FT-IR spectroscopy, FEBS Lett. 505 (2001) 63–67.
[404] P.R. Rich, J. Breton, Attenuated total reflection Fourier transform infrared studies of redox change in bovine cytochrome *c* oxidase: resolution of the redox Fourier transform infrared difference spectrum of heme a_3, Biochemistry 41 (2002) 967–973.
[405] M.W. Calhoun, J.W. Thomas, J.J. Hill, J.P. Hosler, kJ.P. Shapleigh, M.M. J. Tecklenburg, S. Ferguson-Miller, G.T. Babcock, J.O. Alben, R.B. Gennis, Identity of the axial ligand of the high-spin heme in cytochrome oxidase: spectroscopic characterization of mutants in the *bo*-type oxidase of *Escherichia coli* and the aa_3-type oxidase of *Rhodobacter sphaeroides*, Biochemistry 32 (1993) 10905–10911.
[406] R.M. Nyquist, D. Heitbrink, C. Bolwien, R.B. Gennis, J. Heberle, Direct observation of protonation reactions during the catalytic cycle of

cytochrome *c* oxidase, Proc. Natl. Acad. Sci. U. S. A. 100 (2003) 8715–8720.
[407] S. Yoshikawa, K. Shinzawa-Itoh, R. Nakashima, R. Yaono, E. Yamashita, N. Inoue, M. Yao, M.G. Fei, C.P. Libeu, T. Mizushima, H. Yamaguchi, T. Tomizaki, T. Tsukihara, Redox-coupled crystal structural changes in bovine heart cytochrome *c* oxidase, Science 280 (1998) 1723–1729.
[408] P. Hellwig, B. Barquera, R.B. Gennis, Direct evidence for the protonation of aspartate-75, proposed to be at a quinol binding site, upon reduction of cytochrome bo_3 from *Escherichia coli*, Biochemistry 40 (2001) 1077–1082.
[409] P. Hellwig, U. Pfitzner, J. Behr, B. Rost, R.P. Pesavento, W.v. Donk, R.B. Gennis, H. Michel, B. Ludwig, W. Mäntele, Vibrational modes of tyrosines in cytochrome *c* oxidase from *Paracoccus denitrificans*: FTIR and electrochemical studies on Tyr-D4-labeled and on Tyr280His and Tyr35Phe mutant enzymes, Biochemistry 41 (2002) 9116–9125.
[410] F. Tomson, J.A. Bailey, R.B. Gennis, C.J. Unkefer, Z. Li, L.A. Silks, R.A. Martinez, R.J. Donohoe, R.B. Dyer, W.H. Woodruff, Direct infrared detection of the covalently ring linked His–Tyr structure in the active site of the heme-copper oxidases, Biochemistry 41 (2002) 14383–14390.
[411] M. Iwaki, A. Puustinen, M. Wikström, P.R. Rich, Structural and chemical changes of the PM intermediate of *Paracoccus denitrificans* cytochrome *c* oxidase revealed by IR spectroscopy with labeled tyrosines and histidine, Biochemistry 45 (2006) 10873–10885.
[412] M. Iwaki, A. Puustinen, M. Wikström, P.R. Rich, ATR-FTIR spectroscopy and isotope labeling of the P_M intermediate of *Paracoccus denitrificans* cytochrome *c* oxidase, Biochemistry 43 (2004) 14370–14378.
[413] R. Buchet, I. Jona, A. Martonosi, The effect of dicyclohexylcarbodiimide and cyclopiazonic acid on the difference FTIR spectra of sarcoplasmic reticulum induced by photolysis of caged-ATP and caged-Ca^{2+}, Biochim. Biophys. Acta 1104 (1992) 207–214.
[414] R. Buchet, I. Jona, A. Martonosi, Ca^{2+} release from caged-Ca^{2+} alters the FTIR spectrum of sarcoplasmic reticulum, Biochim. Biophys. Acta 1069 (1991) 209–217.
[415] H. Georg, A. Barth, W. Kreutz, F. Siebert, W. Mäntele, Structural changes of sarcoplasmic reticulum Ca^{2+} ATPase upon Ca^{2+} binding studied by simultaneous measurement of infrared absorbance changes and changes of intrinsic protein fluorescence, Biochim. Biophys. Acta 1188 (1994) 139–150.
[416] M. Liu, A. Barth, Mapping nucleotide binding site of calcium ATPase with IR spectroscopy: effects of ATP γ-phosphate binding, Biopolymers (Biospectroscopy) 67 (2002) 267–270.
[417] C. Toyoshima, T. Mizutani, Crystal structure of the calcium pump with a bound ATP analogue, Nature 430 (2004) 529–535.
[418] T.L.-M. Sørensen, J.V. Møller, P. Nissen, Phosphoryl transfer and calcium ion occlusion in the calcium pump, Science 304 (2004) 1672–1675.
[419] T. Kanazawa, P.D. Boyer, Occurrence and characteristics of a rapid exchange of phosphate oxygens catalyzed by sarcoplasmic reticulum vesicles, J. Biol. Chem. 248 (1973) 3163–3172.
[420] A. Barth, Selective monitoring of 3 out of 50,000 protein vibrations, Biopolymers (Biospectroscopy) 67 (2002) 237–241.
[421] I.D. Brown, Chemical and steric constraints in inorganic solids, Acta Cryst. B48 (1992) 553–572.
[422] K. Fahmy, O. Weidlich, M. Engelhard, H. Sigrist, F. Siebert, Aspartic acid-212 of bacteriorhodopsin is ionized in the M and N photocycle intermediates: an FTIR study on specifically ^{13}C-labeled reconstituted purple membranes, Biochemistry 32 (1993) 5862–5869.
[423] Y. Cao, G. Varo, A.L. Klinger, D.M. Czajkowsky, M.S. Braiman, R. Needleman, Proton transfer from Asp-96 to the bacteriorhodopsin Schiff base is caused by a decrease of the pK_a of Asp-96 which follows a protein conformational change, Biochemistry 32 (1993) 1981–1990.
[424] M.S. Braiman, D.M. Briercheck, K.M. Kriger, Modeling vibrational spectra of amino acid side chains in proteins: effects of protonation state, counterion, and solvent on arginine C−N stretch frequencies, J. Phys. Chem., B 103 (1999) 4744–4750.
[425] M. Rudiger, U. Haupts, K. Gerwert, D. Oesterhelt, Chemical reconstitution of a chloride pump inactivated by a single point mutation, EMBO J. 14 (1995) 1599–1606.
[426] K. Hasegawa, T.-A. Ono, T. Noguchi, Vibrational spectra and ab initio DFT calculations of 4-methylimidazole and its different protonation forms: Infrared and Raman markers of the protonation state of a histidine side chain, J. Phys. Chem., B 104 (2000) 4253–4265.
[427] S. Pinchas, I. Laulicht, Infrared Spectra of Labelled Compounds, Academic Press, London, 1971.
[428] N. Johnston, S. Krimm, An infrared study of unordered poly-L-proline in $CaCl_2$ solutions, Biopolymers 10 (1971) 2597–2605.
[429] D.S. Caswell, T.G. Spiro, Proline signals in ultraviolet resonance Raman spectra of proteins: *Cis-trans* isomerism in polyproline and ribonuclease A, J. Am. Chem. Soc. 109 (1987) 2796–2800.
[430] H. Fabian, C. Schultz, J. Backmann, U. Hahn, W. Saenger, H.H. Mantsch, D. Naumann, Impact of point mutations on the structure and thermal stability of ribonuclease T1 in aqueous solution probed by Fourier transform infrared spectroscopy, Biochemistry 33 (1994) 10725–10730.
[431] R.N.A.H. Lewis, R.N. McElhaney, Fourier transform infrared spectroscopy in the study of hydrated lipids and lipid bilayer membranes, in: H.H. Mantsch, D. Chapman (Eds.), Infrared Spectroscopy of Biomolecules, John Wiley & Sons, New York, 1996, pp. 159–202.
[432] P.K. Sengupta, S. Krimm, Vibrational analysis of peptides, polypeptides, and proteins. XXXII. α-poly(L-glutamic acid), Biopolymers 24 (1985) 1479–1491.
[433] S. Pinchas, I. Laulicht, Infrared Spectra of Labelled Compounds, Academic Press, London, 1971.
[434] H. Susi, D.M. Byler, W.V. Gerasimowicz, Vibrational analysis of amino acids: cysteine, serine, ß-chloroalanine, J. Mol. Struct. 102 (1983) 63–79.
[435] P. Dhamelincourt, F.J. Ramirez, Polarized micro-Raman and FT-IR spectra of L-glutamine, Appl. Spectrosc. 47 (1993) 446–451.
[436] K. Gerwert, B. Hess, M. Engelhard, Proline residues undergo structural changes during proton pumping in bacteriorhodopsin, FEBS Lett. 261 (1990) 449–454.
[437] K.J. Rothschild, Y.W. He, D. Gray, P.D. Roepe, S.L. Pelletier, R.S. Brown, J. Herzfeld, Fourier transform infrared evidence for proline structural changes during the bacteriorhodopsin photocycle, Proc. Natl. Acad. Sci. U. S. A. 86 (1989) 9832–9835.
[438] S. Pinchas, I. Laulicht, Infrared Spectra of Labelled Compounds, Academic Press, London, 1971.
[439] C. Madec, J. Lauransan, C. Garrigou-Lagrange, Etude du spectre de vibration de la dl-serine et des ses dérivés deuteries, Can. J. Spectrosc. 23 (1978) 166–172.
[440] A. Lautié, M.F. Lautié, A. Gruger, S.A. Fakhri, Etude par spectrométrie i.r. et Raman de l'indole et de l'indolizine. Liaison hydrogène NH···pi*, Spectrochim. Acta, A Mol. Spectrosc. 36 (1980) 85–94.
[441] H. Takeuchi, I. Harada, Normal coordinate analysis of the indole ring, Spectrochim. Acta, A Mol. Spectrosc. 42 (1986) 1069–1078.
[442] H. Takeuchi, N. Watanabe, I. Harada, Vibrational spectra and normal coordinate analysis of p-cresol and its deuterated analogs, Spectrochim. Acta, A Mol. Spectrosc. 44 (1988) 749–761.
[443] I.P. Gerothanassis, N. Birlirakis, C. Sakarellos, M. Marraud, Solvation state of the Tyr side chain in peptides—An FT IR and O 17 NMR approach, J. Am. Chem. Soc. 114 (1992) 9043–9047.